

Drew University
College of Liberal Arts

Investigation of the Mechanism of Ca²⁺ Catalyzed RNA Phosphodiester Hydrolysis

A Thesis in Chemistry

by

Kyle Messina

Submitted in Partial Fulfillment

of the Requirements

for the Degree of

Bachelor in Arts

With Specialized Honors in Chemistry

May 2014

Abstract

Metal ion catalysis is used in a number of natural enzymes and ribozymes to catalyze phosphodiester cleavage of RNA. Research into metal ion catalysis has been focused on metals such as Zn^{2+} and other transition metals with little emphasis on alkaline earth metals, such as Ca^{2+} due to lower catalytic effects. To elucidate the mechanism of catalysis, an RNA model, 5-Uridine-Guanosine-3' (UpG), was subjected to varying CaCl_2 concentrations at pH 11.5 at 37°C . The R_P and S_P phosphorothioate analogs of UpG (UpsG) were also examined. Solvent deuterium isotope effects were also utilized to determine if the catalytic mechanism proceeded by general acid or general base catalysis. HPLC was used to isolate the stereoisomers previous to kinetic trials and to separate reactants from products in experiment samples.

Catalysis by Ca^{2+} was observed in all models with data normalized to the percent of reactant remaining which was graphed against time to determine the rate constant at each CaCl_2 concentration. The rates for each isomer and the non-thiosubstituted model were then graphed separately against the CaCl_2 concentration and fit to a rectangular hyperbola to determine differences in affinity and rate enhancement. Rate enhancement with Ca^{2+} for UpG was found to be a 326-fold increase, for the R_P isomer a 129-fold increase and for the S_P isomer a 68-fold increase. Initial results seem to indicate that there is minimal loss in affinity when comparing the UpsG models, 0.90 ± 0.09 for the R_P isomer, 0.21 ± 0.09 for the S_P isomer, 0.63 ± 0.35 for the UpG model.

If Ca^{2+} were coordinating with the non-bridging oxygens a substantial loss in affinity should be observed with the thiosubstituted models. Since there is minimal loss in affinity, there may be little to no inner sphere coordination between the Ca^{2+} and non-bridging atoms during hydrolysis. UpG was the chosen model for solvent deuterium

isotope effect studies and the solvent deuterium isotope effect was calculated to be 0.87 in both buffered and non-buffered solutions. This indicates that the mechanism of catalysis does not proceed through general acid/base catalysis.

Acknowledgements

I would like to thank Dr. Cassano for being my research advisor and mentor for 4 years and for helping me to develop into the scientist I am today. I would like to thank my Honors Thesis Committee, Dr. Lantz, Dr. Dunaway and Dr. Surace, for guiding me and assisting me while writing my Thesis. I wish the best of luck and thank Saif Yasin for assisting me in my research and for continuing this research on in my stead. I would also like to thank the Howard Hughes Medical Institute and Drew Summer Science Institute for funding and providing me with the chance to do research at Drew University. Finally I would like to thank my family who has always supported me in all my endeavors.

Table of Contents

Introduction

Biological Foundation- Pg. 1

Preface- Pg. 1

Phosphodiester and their Role in Biology- Pg. 3

Central Dogma of Molecular Biology- Pg. 8

Enzymatic Catalysis- Pg. 10

Catalytic Mechanisms of Nucleases- Pg. 14

What is Phosphodiester Hydrolysis?- Pg. 14

Metal Ion Catalysis- Pg. 18

Catalytic Contribution to Catalysis- Pg. 26

Model Systems- Pg. 29

Emulation of Natural Nucleases: Artificial Nucleases- Pg. 33

Current Research- Pg. 37

Open Questions-Pg. 37

Current Study-Pg. 39

Materials and Methods- Pg 41

Reaction Kinetics-Pg. 41

HPLC Analysis of Reactions-Pg. 42

Results- Pg. 47

Discussion- Pg. 57

General Experiments-Pg.57

Comparison With Ca²⁺ Catalysis of DNA Models-Pg. 61

Bibliography- Pg. 64

Figures

- Figure 1- Complementary Base Pairs, Pg. 3
- Figure 2- Pictorial Representation of DNA and RNA, Pg. 4
- Figure 3- Carbon Esters and Phosphoesters, Pg. 6
- Figure 4- Nucleophiles and the Phosphoester Backbone, Pg. 7
- Figure 5- Central Dogma of Molecular Biology, Pg. 9
- Figure 6- *E. coli* DNA Polymerase 1 Active Site, Pg. 11
- Figure 7- Activation Energy Diagram of Phosphodiester Cleave, Pg. 13
- Figure 8- General RNA Phosphodiester Cleavage, Pg. 15
- Figure 9- General Base and General Acid Catalysis, Pg. 20
- Figure 10- Lewis Acid Coordination of a Metal Ion, Pg. 21
- Figure 11- Catalytic Mechanisms of Alkaline Phosphatase and RNase H, Pg. 23
- Figure 12- Comparison of Activation Energies, Pg. 27
- Figure 13- Example Thiosubstitution of RNA Molecule, Pg. 31
- Figure 14- Pictorial Representation of Artificial Nuclease, Pg. 34
- Figure 15- Organometallic Small Cleaving Molecule, Pg. 36
- Figure 16- UpG and UpsG Models, Pg. 39
- Figure 17- HPLC Plot for 200mM Ca²⁺ Trial, Pg. 48
- Figure 18- Plot of Minutes vs Fraction of UpG, Pg. 49
- Figure 19- Plot of Rate Constant vs Ca²⁺ Concentration of UpG, Pg. 50
- Figure 20- Plot of Log(k) vs pH, Pg. 51
- Figure 21- Plot of Rate Constant vs Ca²⁺ Concentration of UpG and UpsG Trials, Pg. 53
- Figure 22- Plot of Thio effects of Stereoisomers, Pg. 54
- Figure 23- Plot of Time vs. Fraction of UpG for H₂O and D₂O Trials, Pg. 55
- Figure 24- Proposed Mechanism of Ca²⁺ Catalyzed RNA Cleavage, Pg. 57

Tables

- Table 1- Rectangular Hyperbola Fit Data Summary, Pg. 53
- Table 2- UpG Solvent Deuterium Isotope Effects For UpG Cleavage, Pg. 56

Introduction

Biological Foundation

Preface

Deoxyribonucleic (DNA) and ribonucleic acid (RNA) are macromolecules that contain the genetic information of living organisms. These macromolecules are necessary for living organisms since the genetic information is used to produce the structure and maintain the biological functions of living organisms. DNA within living organisms is used as the carrier of genetic information while RNA can be used as an intermediate molecule in protein production or assist in other various biological functions. The genetic code within DNA and RNA is of monumental importance to organisms since subtle changes can easily result in a number of maladies for an organism, including diseases such as cancer. Cancer is a disease that is the result of damage to the DNA either from internal errors during DNA replication or external sources, such as extended exposure to UV-light, where the genetic code is disrupted and normal cellular functions cannot be maintained. Errors that are associated with cancer result in unregulated cell growth and mutations to support the growth of increasing numbers of cancerous cells. Since cancer is only one of many diseases and changes to the genetic code of organisms can produce various effects, research into biological functions and structures of living organisms often focuses on manipulating the DNA and RNA of the organism of interest and observing the changes in the phenotype of the organism. In order to accurately and reliably manipulate DNA and RNA, researchers must first be able to specify their target sequence and then cleave the target sequence efficiently in order to insert their own changes to the genetic code. Currently natural nucleases, molecules that cut DNA and RNA, are used in these studies since they are easily procured from living

cells and can efficiently cut target sequences. These natural nucleases were developed by cells for the purposes of cellular repair, to excise damaged areas of the DNA strand for repair, or to dismantle invading viral DNA or RNA. Many times the mechanisms utilized by natural nucleases are isolated in model systems in an attempt to discern the mechanism of catalysis and the catalytic contribution of individual catalytic strategies. (Rawlings 2006) Currently it is hypothesized that with an increased understanding of the mechanisms of natural nucleases, small molecules can be designed with adapted mechanisms to result in small cleaving molecules that could act as artificial nucleases for research or therapeutic needs. (Feng 2006, Bonfa 2003) Currently natural nucleases are used due to their high efficiency but researchers are limited to cutting select sequences since these molecules developed naturally within organisms and not for research purposes. Although the library of nucleases available to researchers is extensive, the introduction of custom nucleases that cleave as efficiently as natural nucleases would allow researchers to have an even greater variety of choice when conducting experiments. Researchers have also hypothesized that these small molecules could be developed and utilized in medical therapies for treatment of certain diseases such as leukemia. (Murtola 2008, Feng 2006, Bonfa 2003) Leukemia is the result of over expression of certain genes that results in excessive mRNA. Theoretically if one was able to target and cleave the over expressed mRNA, one could mitigate the disease and slow the spread. This type of treatment would require advanced artificial nucleases that have the specificity to target only the offending molecule and efficiency to cleave the molecule to have an impact. In order to develop these artificial nucleases, it is important to understand the characteristics of DNA and RNA and why these nucleases were developed.

Phosphodiesters and their Role in Biology

The sequential ordering of the nucleotides determines the genetic information that is encoded into that specific strand of DNA or RNA. The nucleotides are made of a nitrogen heterocyclic base (nucleobase), a pentose sugar and a phosphate residue. (Figure 1) DNA contains the sugar deoxyribose and can be comprised of adenine (A), guanine (G), cytosine (C) and thymine (T) for nitrogen bases. RNA, on the other hand, contains the sugar ribose and contains the nitrogen bases of adenine, guanine, cytosine and uracil (U). In both DNA and RNA, the nucleotides are arranged in repetitious format with each

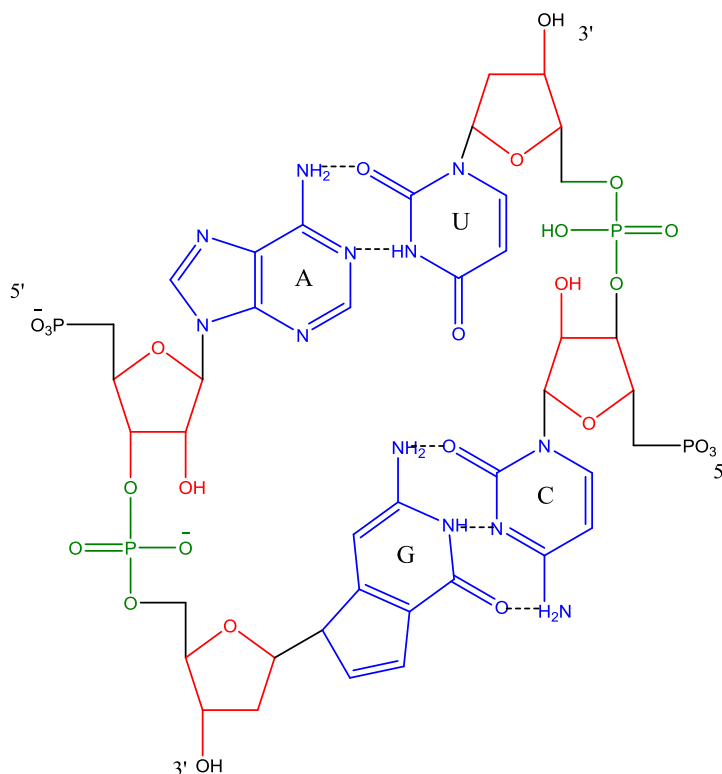


Figure 1: Picture of nucleotides with possible nucleobases. Nucleotides are made of a nitrogen heterocyclic base (blue), a pentose sugar (red) and a phosphate residue (green). The pentose sugar base remains a constant along with the phosphate residue. The nitrogen heterocyclic base can be any of the molecules labeled in blue. For RNA, as pictured, these nucleobases include adenine (A), uracil (U), guanine (G) and cytosine (C) and are paired with their complementary base pairs. 5' and 3' ends are marked on both strands.

sugar interacting with another sugar. These sugars are arranged so the nucleobases face opposite of the phosphodiester bond. (Figure 1) The overall structure of DNA is a double-stranded structure where the nucleobase portion of the nucleotide engages in hydrogen bonding with a respective base pair, adenine and thymine or guanine and cytosine. (Figure 2) The strands of DNA run opposite of the other with one strand running 3' to 5' with respect to the sugar and the other running 5' to 3', the same as the RNA shown in Figure 1. (Pinjari 2008) RNA's structure is similar to that of DNA except that RNA is typically a single strand but can engage in base pairing like DNA depending on the structure and type of RNA synthesized. (Blackburn 1990) As one might expect, these differences in structure between DNA and RNA have relegated them into different tasks within organisms.

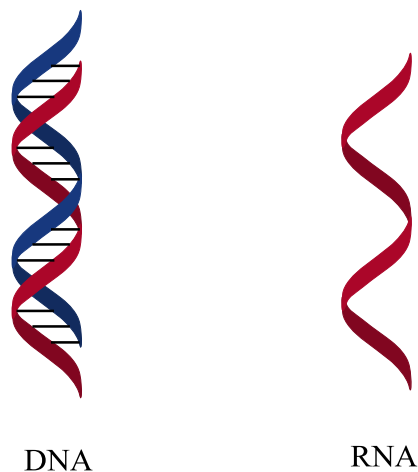


Figure 2: Simple pictorial representation of DNA and RNA. DNA is a double-stranded molecule with the nucleobases of each strand interacting while RNA is single-stranded with ability to engage in base pairing.

DNA's double stranded structure and greater stability is exploited for the long term storage of genetic information within an organism and has a more prominent role in the cell. RNA is much shorter lived when compared to DNA and is relegated to the role

of an intermediate where storage of information is needed only until the biological function is accomplished. Although there is a difference between the stability of DNA and RNA, both must have great enough stability so that the encoded information does not degrade or become inaccurate. When compared to typical lifespans of organism, the half-lives of DNA and RNA are astounding with the half-life of DNA and RNA, at 25°C and neutral pH, equal to 140,000 years and 110 years respectively. (Bonfa 2003, Schroeder 2005) Macromolecules also assist in maintaining the structure of DNA and RNA, repairing damage caused by molecules, further extending the life of DNA and RNA and minimizing damage. The secret to the stability of DNA and RNA lies in the genetic “tape” that links the nucleobases together, the phosphodiester bond. (Westheimer 1987)

Phosphodiester bonds are located between sugar bases and act as the “tape” which secures and links the nucleotides together. (Westheimer 1987) Phosphodiester bonds are located in both DNA and RNA and form a backbone to both nucleic acid structures appearing between the sugar bases and going down the length of the macromolecule. (Figure 1) The name phosphodiester comes from the fact that a phosphodiester is analogous to an ester bond except that the carbon center is replaced with phosphorus. Because phosphorous forms bonds with four oxygen atoms in a structure, it can form up to three analogous esters bonds, seen in Figure 3. (Blackburn 1990) In the case of DNA and RNA, only two ester bonds form and so it is known as a diester which is the molecule labeled C in Figure 3. The unique structure of phosphodiester bonds allows for the linkage of nucleotide monomers to form DNA and RNA. (Westheimer 1987) The phosphodiester bond also causes the formation of a

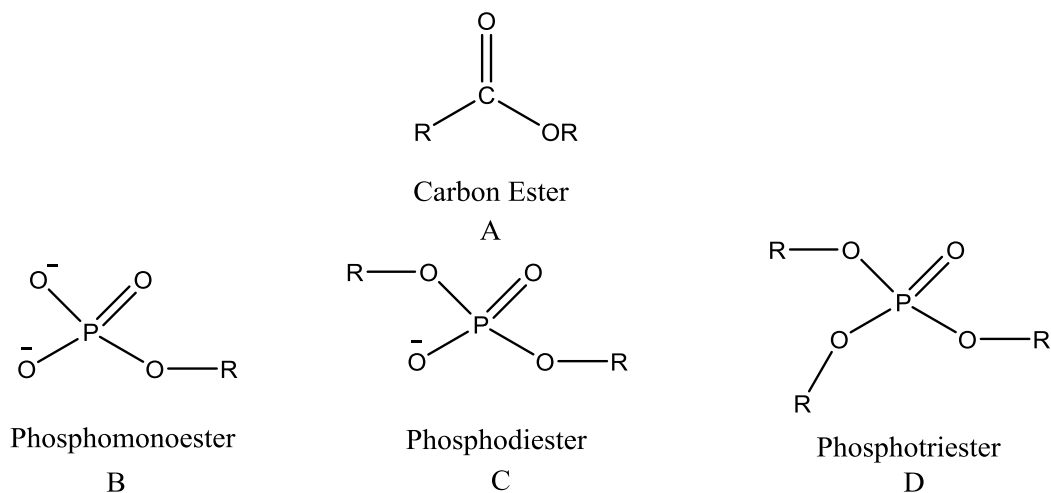


Figure 3: Examples of an ester and phosphoester bonds with R representing generic carbon groups. Example A is a simple carbon ester which consists of a carbonyl group and an oxygen bonded to a general organic group, denoted by R. Examples, B, C and D are various phosphoester bonds which are denoted as monoester (B), diester (C) and triester (D). These names are derived based on the number of R groups bonded to the oxygen atoms.

negative charge to develop on the non-bridging oxygen atoms which contributes significantly to the chemistry of DNA and RNA as shown in Figure 3. (Westheimer 1987) Normally an atom like phosphorus that is surrounded by a number of electronegative atoms gains a positive charge and is vulnerable to attack by negatively charged nucleophiles. A phenomenon occurs, similar to magnetism, where like charged substances repel and so negatively charged nucleophiles are blocked from attacking the phosphorus by the negatively charged non-bridging oxygen atoms. The negative charge acts as a deterrent, lowering the number of successful attacks on the nucleophile and limiting the rate of phosphodiester breakdown, illustrated in Figure 4. (Westheimer 1987) If the nucleophiles cannot attack the phosphorus, the chance of breakdown is significantly lowered which aids in the stability of DNA and RNA.

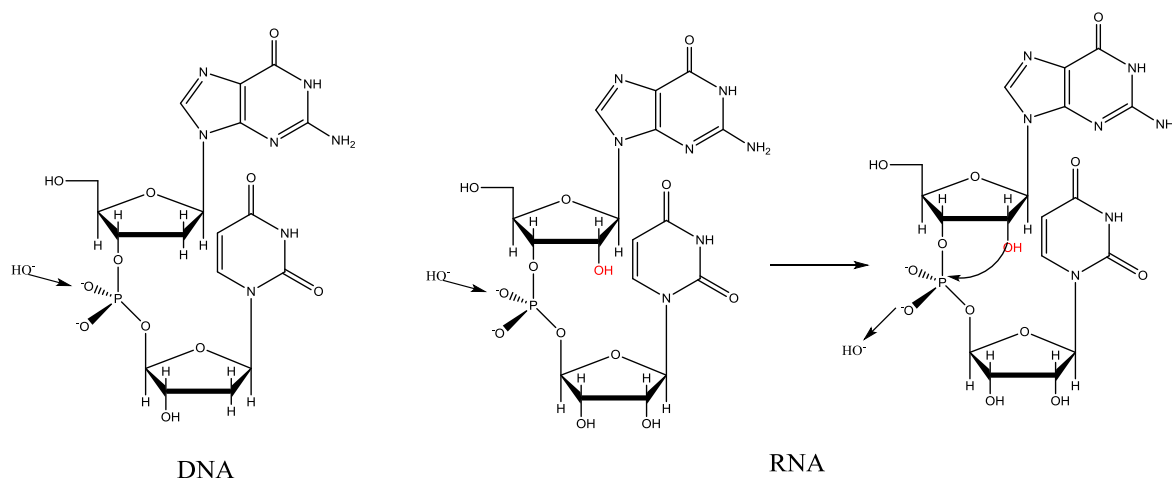


Figure 4: Repulsion of external nucleophile by phosphodiester backbone. The phosphodiester backbone of both DNA and RNA, pictured here, contain negatively charged oxygen atoms. Nucleophiles are also negatively charged and are repelled by the negatively charged backbone. In the case of RNA, the 2' hydroxyl group (red) can avoid the non-bridging oxygen atoms and can initiate an attack on the phosphorus.

Admittedly this does not explain the difference between the 140,000 and 110 year half lives of DNA and RNA. (Bonfa 2003, Schroeder 2005) One of the keys to the difference between the half lives of DNA and RNA is the structure of the sugar base. The deoxyribose in DNA lacks the 2' hydroxyl group that is present in the RNA ribose structure. (Westheimer 1987, Li 1999) The 2' hydroxyl group can potentially be deprotonated in solution and would gain a negative charge which allows the hydroxyl group to function as a nucleophile. (Westheimer 1987) As observed in Figure 4, the hydroxyl group is positioned away from the negatively charged oxygen atoms; bypassing the major defense against breakdown. In addition the hydroxyl group is in close proximity of the phosphodiester bond, increasing the chance of attack on the phosphorus. (Westheimer 1987) Both of these situations, in conjunction with each other, result in a much greater chance of a nucleophile reaching the phosphorus which results in a much

greater chance of breakdown. As mentioned previously, DNA and RNA due to their stability, store the genetic information for organisms in a sequence of nucleotides. How does storing the information in a sequence of molecules result in the vast amount of biological activity within an organism?

Central Dogma of Molecular Biology

DNA's and RNA's main purpose within biological organisms is to act as a template from which proteins, macromolecules that assist in the various functions with the cell or organism, are produced. Both DNA and RNA are used in conjunction for the production of proteins, starting from the transcription of DNA into mRNA, a type of RNA which acts as temporary storage. The process of transcription is highly regulated to ensure that transcription only occurs when the production of a protein is necessary. Promoter sequences, a specific series of nucleotides, located on the DNA are responsible for initiating transcription and are where the regulation occurs. Transcription begins when RNA polymerase, a protein, attaches itself to the promoter sequence and goes along the DNA strand to transcribe the DNA sequence into an mRNA sequence. Each nucleotide in the DNA strand is matched to its base pair complement in the RNA strand; adenine with thymine/uracil, guanine with cytosine. (Blackburn 1990) Cytosine is the only exception to this rule and is transcribed as uracil in the mRNA strand. In eukaryotes the mRNA sequence is subjected to post-transcriptional changes where sequences of RNA known as introns are spliced out of the mRNA sequence to produce a mature mRNA product. This process, known as splicing, produces a mature mRNA molecule that is then used in the proceeding steps of protein synthesis.

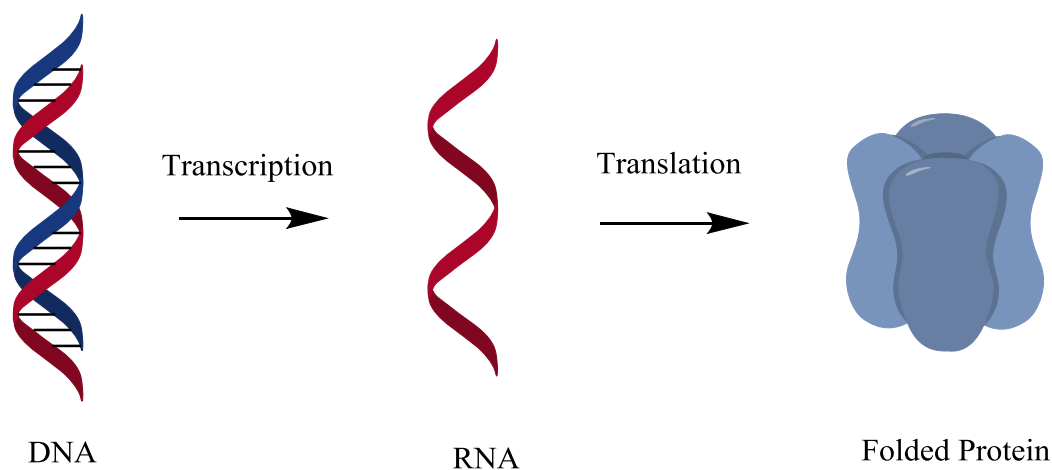


Figure 5: Pictorial representation of the molecular dogma of biology. DNA acts as a template and is first transcribed into RNA. The RNA strand is then read as a series of codons which give instructions on the necessary amino acids to form a protein. The protein then becomes a string of amino acids and will fold into a 3D assembly.

The mRNA is then directed to an organelle known as a ribosome within the cell where translation of the mRNA into protein actually occurs. The ribosome binds to a nucleic acid sequence on the mRNA known as the initiation site to begin. Once translation is initiated the ribosome reads the mRNA as a series of codons, a sequence of three nucleic acids that codes for one of 20 amino acids, and a string of amino acids is bonded together by the ribosome. (Blackburn 1990) Once all the amino acids are bonded together, the protein will begin to fold from a “string” of amino acids into a 3D conglomeration. The shape and size of the 3D conglomeration of amino acids can have varying functionalities that change depending on the order and which amino acids it consists of.

The 3D conglomeration of amino acids is known by the general term protein, which is used to describe a collection of amino acids that form one molecule and performs a function within a cell. Some proteins act as relatively static structures within the fluid membranes of cells while others take a direct part in a cell’s biochemical

reactions. For example, hemoglobin is a relatively static protein that binds oxygen in high oxygen environments and unbinds in low oxygen environments. Some proteins, such as nucleases, can engage with DNA and RNA molecules to cut them at specific points. Proteins which catalyze reactions are a specific class of protein known as an enzyme. Many chemical reactions that are required to sustain life within an organism naturally occur at a rate that is significantly slower than what is required to sustain biological functions. Enzymes significantly increase the rate of a reaction so that the chemical reaction occurs on the proper time scale. Although there is a myriad number of reactions that must occur within cells which require innumerable reactants, there are a number of characteristics that are inherent to all enzymes.

Enzymatic Catalysis

In order to induce catalysis, enzymes share two necessary characteristics: their specificity and an active site. Specificity refers to the ability of an enzyme to bind to one or a handful of specific molecules, known as substrates. The specificity of an enzyme depends on the amino acids present within the enzyme, with different charges and shapes giving different preferences for what molecules can bind. The different properties and arrangements of the amino acids allow for specific substrates to bind in a variety of ways to the enzyme. Typically the enzymes will bind in a portion of the molecule known as the active site. The active site of the enzyme is where the reaction physically occurs and an example is illustrated in Figure 6. There are a number of catalytic strategies that enzymes can utilize to induce catalysis and many of them revolve around two specific concepts: proximity of the substrates to each other and lowering the activation energy of

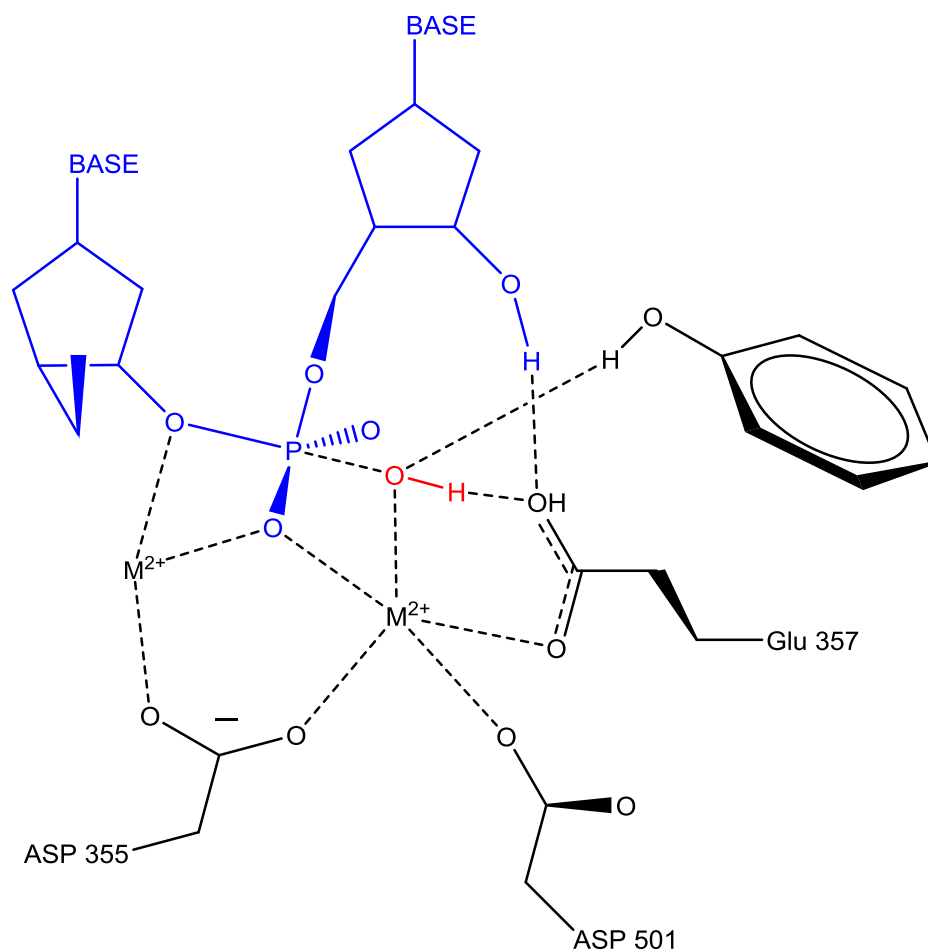


Figure 6: Example of a nuclease active site where Asp 355, Asp 501 and Glu 357 are amino acids that are part of a larger enzyme, not pictured due to size constraints. The amino acids interact with the target nucleic acid (blue) or the nucleophile (red). The nucleophile is positioned at an optimal angle to attack the phosphorus by the various residues and metal ions. The “M” represents general metal ions which assist in the formation of the nucleophile and stabilize growing negative charge on the non-bridging oxygen atoms or the oxygen atom of the leaving group. Adapted from Beese 1991.

the reaction. Having the substrates near each other is logical since if the substrates are separated by distance the chance of the two substrates interacting is significantly lowered. This is similar to RNA where the proximity of the 2'-hydroxyl group to the phosphodiester bond increases the chance of cleavage occurring thus lowering the half-life of RNA. Hence that is why the substrates are attracted and bound to the active site, often in a place that sets up the substrates in orientations appropriate for the reaction.

Lowering the activation energy of a reaction is the main way to increase the rate of a reaction. One can think of it as making a hill on a walking path smaller; it takes less energy to walk up the hill and so one is more likely to get over the hill. A chemical reaction typically proceeds in a manner in which the two substrates are brought together and react to give a product. In regards to the hydrolysis of DNA, the DNA and a hydroxide molecule are the substrates. (Cassano 2002) A hydrolytic enzyme positions the hydroxide to attack the phosphodiester bond, and when the attack occurs a transition state between the DNA and the hydroxide molecule occurs. This transition state is a structure between reactants and the products. This transition state is also high in energy compared to the reactants and products, making it unfavorable to form and inherently unstable. However the transition state must be reached by the reactants for the formation of the product. This is because when the molecule proceeds through the transition state, the molecule will be in a more favorable and lower energy state. The energy needed to form the transition state is known as the activation energy and the lower the activation energy, the easier and faster it is to reach the transition state. An example of an activation energy diagram is shown in Figure 7 and shows a generic phosphodiester hydrolysis reaction going from reactant to an intermediate to the product.

When an enzyme lowers the activation energy needed to reach the transition state, the reaction is much more likely to proceed to the product. For example, the rate of DNA cleavage in biological systems can be increased by up to 10^{17} fold with cleavage happening in seconds. (Bonfa 2003) Although it is important for DNA and RNA to remain stable over long periods of time, there are situations which arise when the stability of nucleic acids is a detriment. (Pinjari 2008) If damage occurs to a specific base pair or

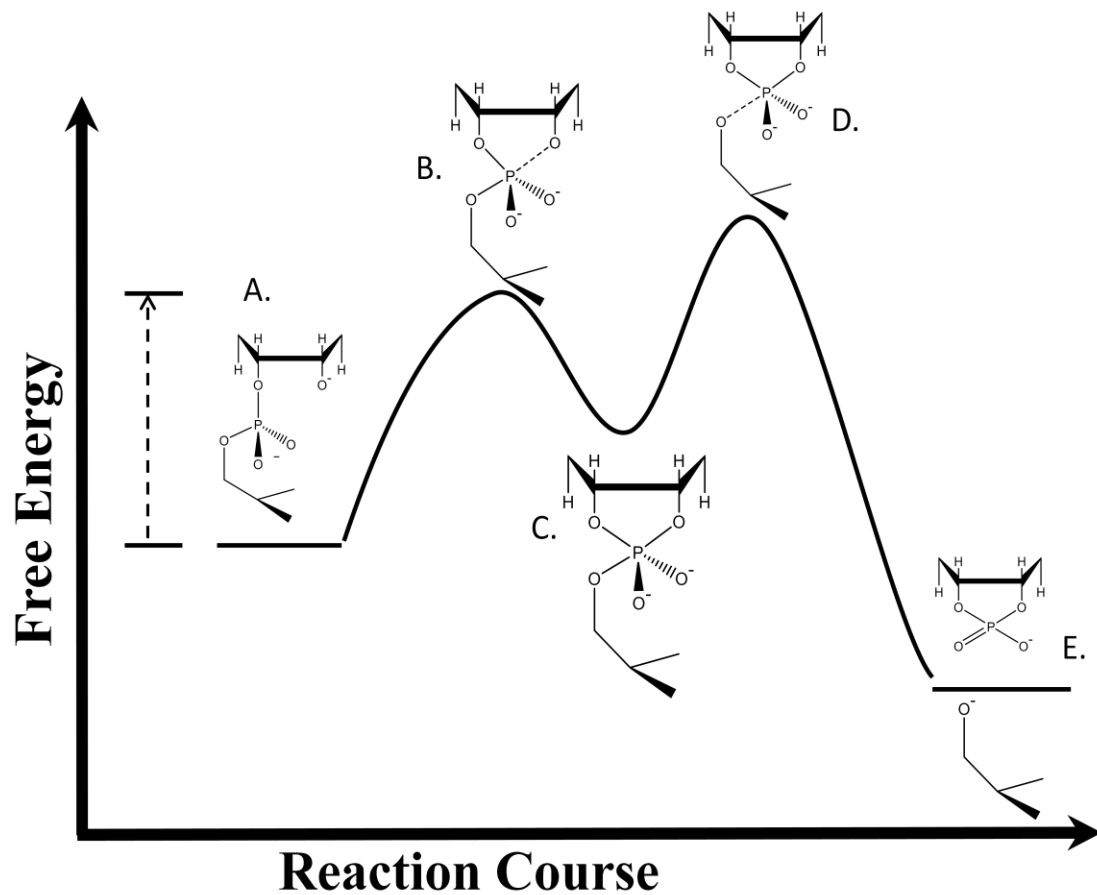


Figure 7: Example of an activation energy diagram for phosphodiester hydrolysis. Reactants, labeled A, appear on the left flat line and products, labeled E, appear on the right flat line. In order to proceed from reactant to product, the reactants must acquire enough energy to reach the transition state, labeled as B and D, known as the activation energy barrier. The activation energy barrier is the difference in energy between the minimums, A and C and the transition states, labeled B and D. An example activation energy is labeled as AE. Intermediates, labeled C, are structures that are stable and last for an observable period of time before proceeding to the product.

mismatching of base pairs occurs during DNA replication, there needs to be a cellular process to allow for the breakdown of the damaged section for repair. (Pinjari 2008)

Otherwise these errors may result in the new cell being unable to reproduce and pass on genetic information. (Westheimer 1987) Similarly there are situations that call for the breakdown of RNA. If a coded protein is present at high enough levels, cleaving the RNA would result in reduced expression of the protein. In both cases, cells utilize

enzymes known as phosphodiesterases or nucleases to increase the rate of breakdown of phosphodiester bonds through hydrolysis. (Pinjari 2008) Enzymes that facilitate the breakdown of nucleic acids contain a diverse number of mechanisms that are highly efficient in catalyzing this reaction.

Catalytic Mechanisms of Nucleases

What is Phosphodiester Hydrolysis?

In order to understand how enzymes stabilize the transition state and facilitate hydrolysis it is best to understand how hydrolysis occurs and what the transition states are. Mechanistic studies utilizing heavy atom isotope effects have elucidated various aspects of phosphodiester hydrolysis in both non-enzymatic and enzymatic reactions. (Cassano 2004, Harris 2010) Heavy atom isotope effects (HAIE) involve the replacement of a target atom with a heavier isotope in order to cause a change in the stiffness of the bonding environment. (Cassano 2004) This information is useful in determination of when and if bond formation occurs during phosphodiester hydrolysis. Mechanistic studies are based on the fact that phosphodiester hydrolysis proceeds through an SN₂ reaction where the nucleophile attacks the phosphate and can occur as either a step-wise or concerted mechanism. (Hengge 1991, Cassano 2004) In the concerted mechanism, the reaction takes place in a single step where the attack of the nucleophile and the departure of the leaving group occur simultaneously. (Cassano 2004) In the step-wise mechanism, the formation of a phosphorane intermediate occurs before proceeding into the departure of the leaving group. (Cassano 2004) The phosphorane forms in both types of mechanisms but is short lived during the concerted mechanism due to the instability of the molecule. (Figure 8) Additional information can also be obtained by looking at the B-

Leaving Group (B_{LG}) values which are a measure of the sensitivity to the reactivity of the leaving group. B_{LG} values that are increasingly negative indicate a more associative transition state, resembling a triester or phosphorane, while more positive values indicate a relatively loose transition state, resembling a monoester.

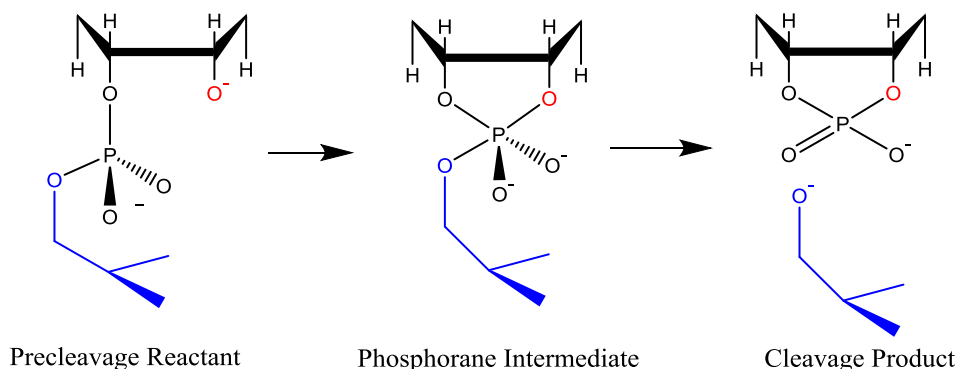


Figure 8: A general reaction scheme for the phosphodiester hydrolysis of RNA with the 2' hydroxyl group (red) acting as the nucleophile. The 2' hydroxyl group attacks the phosphorus and causes the formation of the phosphorane intermediate, middle molecule, and displacement of the resonance stabilized double bond to the non-bridging oxygen atoms, labeled A. Upon reformation of the double bond the leaving group (blue) is then displaced forming a cyclic product.

The mechanism of phosphodiester hydrolysis has been thoroughly researched over the years with simple phosphate esters to determine how the reaction proceeds. It has been determined that varying the environment around the reactant can have a large effect on whether the mechanism is concerted or step-wise. (Korhonen 2012, Mikkola 1999, Harris 2010, Virtanen 2004) At basic pH's a concerted mechanism is observed due to the instability of the phosphorane intermediate and only basic cleavage occurs. (Mikkola 2013) This can be observed when looking at studies such as Harris, et. al. 2010 where the hydrolysis of a simple dinucleotide model, Uridine monophosphate Guanosine (UpG), was monitored at highly basic pH's using Kinetic Isotope Effects (KIE). KIE experiments use the rate difference between heavier and lighter isotope samples to test

mechanistic hypothesizes. Heavier isotopes prefer bond formation while lighter isotopes prefer bond cleavage. In these conditions it was found that cleavage occurred through a concerted mechanism and that the transition state appeared more product-like. At acidic or neutral pH's, phosphodiester hydrolysis proceeds through a stepwise mechanism with a longer-lived phosphorane intermediate resulting in both general cleavage and isomerization of the phosphorane intermediate. (Mikkola 1999, Mikkola 2013) This can be observed in the Mikkola, et. al. 1999 study where the cleavage of RNA models with differing leaving groups were observed in acidic conditions. During the uncatalyzed portion of the study, products associated with a step-wise mechanism were observed, specifically products from isomerization due to pseudorotation and cleavage. (Mikkola 1999) For reactions where uncatalyzed phosphodiester hydrolysis is occurring, the observations appear true over a wide range of reactants and models. Even between model systems used for RNA or DNA, these generalizations remain true with a step-wise mechanism being present in acidic conditions and a concerted mechanism in basic conditions. However once additional variables are considered, these observations begin to break down. As additional variables are added to the system such as buffer solutions and metal ions, the systems become increasingly complex and are much more likely to deviate from these general observations.

The addition of metal ions often tends to cause the mechanism of phosphodiester hydrolysis to become altered because of the association of metal ions with the transition state. The basis for the changes to the transition state cannot be generalized as easily as the acidic and basic environments due to the varying properties of metal ions. Although most metal ions appear to push the transition state towards a product-like intermediate or

a step-wise mechanism. In a 2008 study conducted by Humphry, a complex containing two Zn^{2+} ions was introduced to an HpPNP phosphate ester model to see how the mechanism was affected in the presence of Zn^{2+} . Through KIE's it was determined that the presence of a Zn^{2+} catalyst pushed the transition state to a more advanced state of bond formation to the phosphorus and increased bond fission to the leaving group. (Humphry 2008) This study was conducted following an experiment in which a Co^{3+} catalyst was introduced to a pNPP phosphate ester model, which when uncatalyzed has a concerted mechanism with little bond formation and little bond cleavage. (Humphry 2002) The introduction of a Co^{3+} containing complex not only catalyzed the reaction but caused cleavage to become a step-wise mechanism with a very late transition state. (Humphrey 2002) One reason for this effect is that metal ions may provide increased stabilization to the phosphorane intermediate allowing for a longer lived state. (Humphry 2008) Not all metal ions are created equally. While all metal ions have positive charge, their size and charge density are varied and so simple generalizations between all metal ions cannot be made easily. As described previously, the metals ions developed differing positive charges, +2 and +3, in addition to the Co^{3+} pushing a phosphodiester model closer to a later transition state. Similarly, more complex systems with greater numbers of variables cannot be easily generalized with simple rules, yet the production of effective artificial nucleases depends on knowing how phosphodiester hydrolysis is affected in complex biological systems. Therefore, numerous types of system must be studied in order to elucidate how phosphodiester hydrolysis can be affected in increasingly complex systems.

In order to design effective small cleaving molecules, it is imperative to understand how the transition states of molecules vary under a number of uncatalyzed and catalyzed conditions. The main purpose of an enzyme is to ease the formation of the transition state during a reaction and so natural enzymes are a prime focus of research. Enzymes have the specificity necessary to bind the non-transition state molecules, in addition to stabilizing the formation of the transition state. Due to these properties many researchers have conducted research on the catalytic strategies of enzymes in order to learn methods of catalysis for further analysis.

Metal Ion Catalysis

Natural nucleases are the perfect sources of catalytic mechanisms for phosphodiester cleavage due to their enormous catalytic potential. As mentioned before, some nucleases can induce 10^{17} -fold increases in rate, cleaving phosphodiester bonds in seconds. (Bonfa 2003) This is also the main reason why many phosphodiester model systems attempt to emulate enzymatic forms of catalysis. The most prominent and usually necessary form of catalysis used by enzymes in phosphodiester hydrolysis is known as metal ion catalysis. (Imohof 2009) Metal ion catalysis is a general term that describes when a metal ion is used in some capacity to catalyze a cellular process. There is no specific number of metal ions that are associated with metal ion catalysis but one, two or three metal ions can be used by a single enzyme. (Pinjari 2006) The term metal ion catalysis includes such processes as general acid/base catalysis or Lewis acid catalysis. (Ku 2002)

General base catalysis is a catalytic process in which a molecule assists directly in the deprotonation of a select molecule. (Figure 9) (Imohof 2009) This is the most probable form of metal ion catalysis in EcoRV, a bacterial enzyme, where an Mg^{2+} ion positions an aspartate residue to accept a proton from a water molecule to act as the nucleophile. (Imohof 2009) General acid catalysis occurs when the metal ion assists in the protonation of a select molecule. (Figure 9) General acid catalysis can be utilized to help facilitate the departure of the 5'-O leaving group to complete phosphodiester hydrolysis. (Wong 2011) This process occurs within the hammerhead ribozyme, where a guanine residue participates in the general acid catalysis and donates to the leaving group. (Wong 2011) General acid and general base catalysis are not unique to metal ions and are strategies that are present in number of enzymes. General acid and general base catalysis are most often associated with the residues associated with enzymatic catalysis and it is less common for metal ions to participate in these forms of catalysis. It is often the case that general acid and general base catalysis involve a number of amino acid residues working in concert with one another to facilitate a proton transfer.

Metal ion catalysis is often associated with the metal ion acting as a Lewis acid, a substance that can accept an electron, and conducting catalysis through direct interactions, as shown in Figure 10. Many enzymes associated with RNA/DNA phosphodiester hydrolysis utilize many ions ability to act as a Lewis acid. (Imohof 2008, Ku 2002) The positive charge carried by metal ions is what allows for metal ions to act as a Lewis acid and accept negative charge from a variety of sources. One mechanism that is

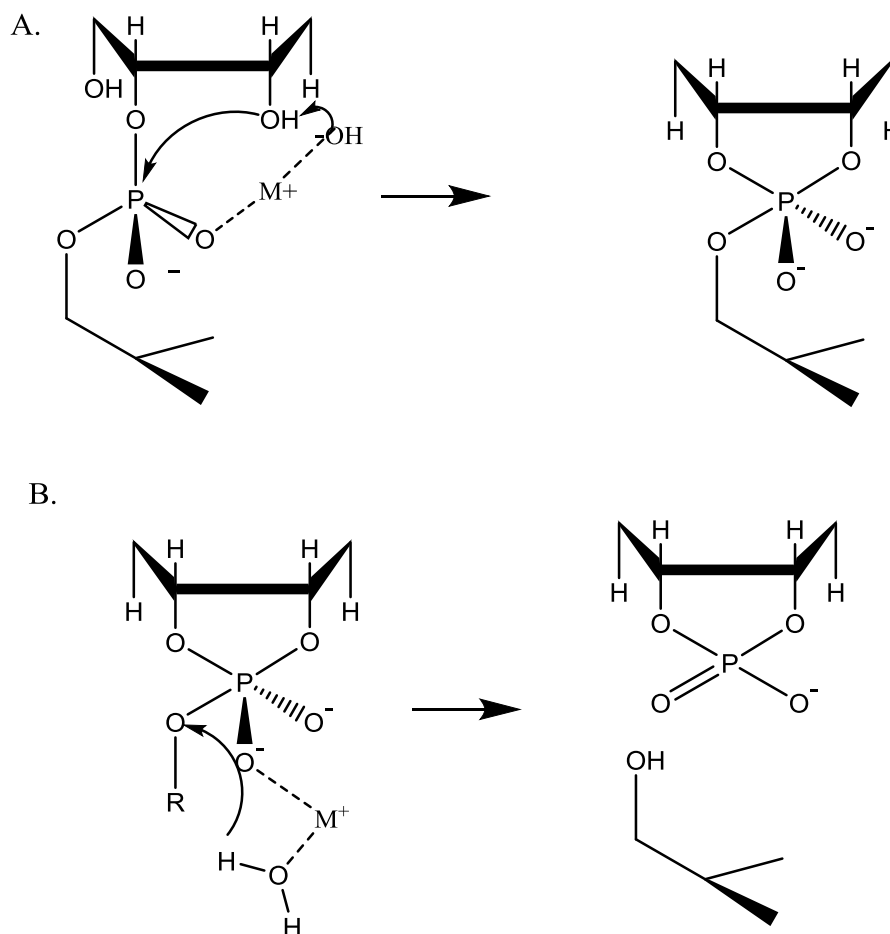


Figure 9: Mechanisms of general base, labeled A, and general acid catalysis, labeled B. In general base catalysis, the metal ion, labeled M^+ , assists in the deprotonation of a molecule by using another molecule such as a hydroxide deprotonating the 2' hydroxyl. In General Acid catalysis, the metal ion assists in the protonation of a molecule, such as the protonation of the leaving group. Leaving group is replaced by an R group in B for clarity.

possible is the activation of the nucleophile through direct interaction. (Golden 2011, Chen 2010) This is observed in the HDV ribozyme, a catalytic RNA, where the Mg^{2+} metal ion facilitates the deprotonation of the 2' hydroxyl group which then activates the 2' hydroxyl for attack. This strategy is used to increase the likelihood of hydrolysis starting by priming and preparing a nucleophile instead of waiting for the 2' hydroxyl to be deprotonated or for a hydroxide molecule to make it past the non-bridging oxygen atoms.

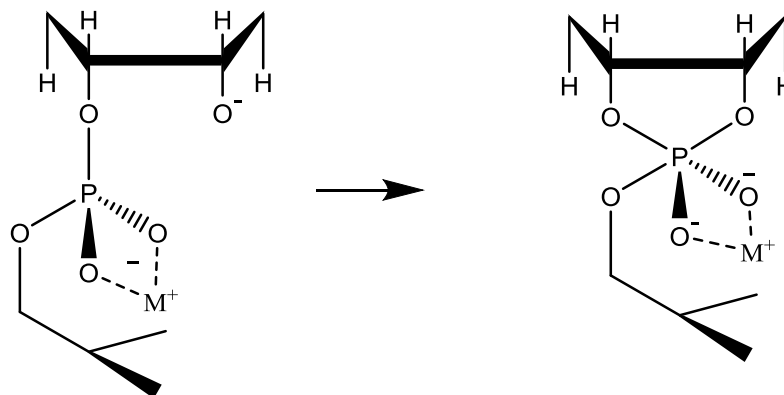


Figure 10: Example of Lewis acid catalysis where a metal ion coordinates with a molecule, the non-bridging oxygen atoms in this case, to stabilize negative charge on a molecule.

By preparing and ensuring the 2' hydroxyl group and hydroxide remain deprotonated, hydrolysis is much more likely to occur.

As previously mentioned, the main purpose of enzyme catalysis is used to facilitate the formation of the transition state. This is why the other primary strategy used is the electrostatic stabilization of the transition state by positioning metal ions near areas of growing negative charge such as the non-bridging oxygen atoms of the phosphodiester bond. For example, the hammerhead ribozyme catalyzes the self-cleavage of RNA through electrostatic stabilization. (Wong 2011) The Mg^{2+} ion stabilizes the formation of the nucleophile by following the negative charge during the phosphoryl transfer step and providing electrostatic stabilization to the nucleophile. Similarly in the endonuclease domain of colicin E7, from *E. coli*, there is a single zinc ion that is hypothesized to be used to stabilize the phosphoanion transition state through electrostatic stabilization. (Ku 2002) In phosphodiester hydrolysis it is unfavorable for the excess negative charge to be displaced onto the non-bridging oxygen atoms and consequently raises the energy needed to form the transition state. This is where the ability of metal ions to act as a Lewis acid

can assist; absorbing the excess negative charge and increasing the chance of reaching the transition state. The use of one metal ion can be beneficial for the formation of the transition state and greatly ease the formation of the transition state. So, would the use of multiple metal ions further decrease the unfavorability of forming the transition state?

As it turns out, the use of one metal ion for phosphodiester hydrolysis is the more unusual form of catalysis since most nucleases have developed to use two metal ions. Increasing the number of metal ions within an enzyme allows for a greater variety of catalytic strategies to be utilized. With an additional metal ion, more excess negative charge can be further suppressed in one area of the molecule. This use of two metal ions can be observed for both DNA and RNA phosphodiester hydrolysis in *E. coli* alkaline phosphatase and RNase H. (Figure 11) (Holtz 1999, Nowotny 2005) Alkaline phosphatase uses the metal ions to add both specificity to the active site and to catalyze phosphodiester hydrolysis. (Holtz 1999) The zinc ions are positioned to be able to interact with one non-bridging oxygen atom each and position the scissile phosphate, the phosphate that will be attacked, for an attack by a nucleophile. Then one zinc atom will coordinate a hydroxide to attack as a nucleophile and facilitate the attack on the scissile phosphate. (Holtz 1999) In the case of RNase H, two magnesium ions are used in the place of zinc ions and interact similarly with the non-bridging oxygen atoms and direct a nucleophile to attack the scissile phosphate, Figure 11. (Nowotny 2005) In addition both magnesium ions interact with one of the non-bridging oxygen atoms and provide electrostatic stabilization to the transition state. (Nowotny 2005) This catalytic strategy may have developed for substrates where negative charge built up on the non-bridging oxygen atoms to a greater extent than on the leaving group. So instead of placing metal

ions in different areas of growing negative charge, the metal ions were concentrated in one area to decrease the excessive negative charge. Many of the previous examples involved excess negative charge being present on only non-bridging oxygen atoms yet this phenomenon is present on another area during phosphodiester hydrolysis.

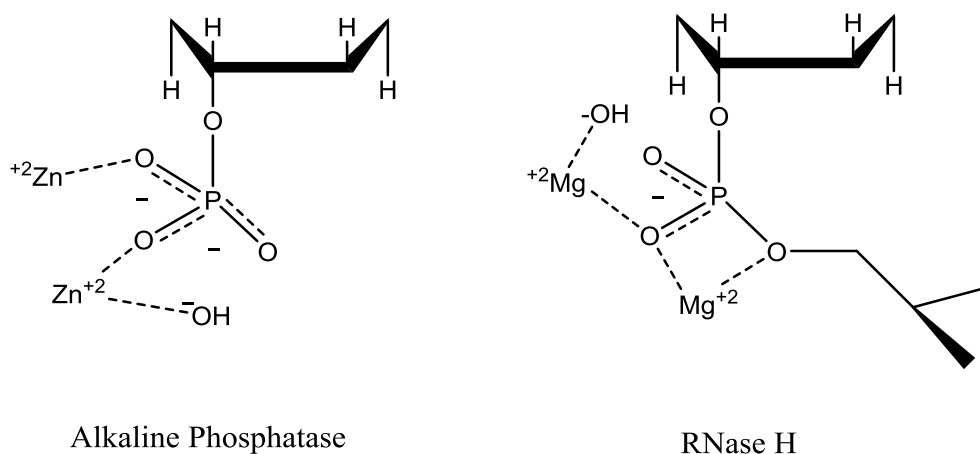


Figure 11: Figure of Alkaline Phosphatase and RNase H mechanisms. In the case of alkaline phosphatase, two Zn^{2+} ions are utilized with one associating with only single non-bridging oxygen atom and the other ion associating with the other non-bridging oxygen atom and directing the nucleophile, hydroxide. With RNase H, two Mg^{2+} ions are utilized with both ions associating with one non-bridging oxygen atom. Each ion also either coordinates or directs the nucleophile, hydroxide, or associates with the oxygen atom on the leaving group.

As phosphodiester hydrolysis occurs excess negative charge also begins to build up on the leaving group as bond fission occurs between the phosphorus and the bridging oxygen atom. The catalytic strategies of some enzymes use metal ions to stabilize the negative charge growth on the leaving group further diversifying the number of catalytic strategies. This catalytic strategy is present in DNA polymerase I adding further to the variety of catalytic mechanisms. (Beese 1991) Both metal ions, A and B, interact with one of the non-bridging oxygen atoms of the phosphodiester bond as illustrated in Figure 6. (Beese 1991) The A interacts with a hydroxide molecule to stabilize the formation of

the nucleophile and to orientate the hydroxide to attack the phosphodiester bond. B interacts with the leaving group and provides electrostatic stabilization as the leaving group gains a negative charge from the additional electrons. (Beese 1991) Ribonuclease H is also theorized to use two Mg^{2+} ions to promote nucleophile formation and stabilize the formation of the leaving group with one metal ion being associated with each process, shown in Figure 11. (Vivo 2008) It is important to note that enzymes are not static structures and have the ability to adjust their structure as a reaction occurs. The primary purpose of having a dynamic structure is to adjust to the changing conditions of the reaction and stabilize not just the initial structure but various structures associated with the reaction.

As the reaction proceeds further toward the product and the phosphorane intermediate begins to form, the metal ions of Ribonuclease H migrate closer to each other and stabilize the non-bridging oxygen atoms of the phosphorane intermediate. (Vivo 2008) Enzymes such as Ribonuclease H, not only add to the range of possible mechanisms but remind researchers that many methods used such as X-ray crystallography, which is used to elucidate how metal ions are positioned, only show a static structure. It is quite possible that many of the mechanisms mentioned may be more complex than first interpreted but the full scope of how metal ions are utilized is limited since only snapshots of the positions of metal ions are seen. What is consistent is that the use of metal ion catalysis as a catalytic strategy is prevalent among nucleases for both DNA and RNA.

The reason for the prevalence of metal ions in phosphodiester hydrolysis is due to the versatility of metal ions within the environment that is produced during

phosphodiester hydrolysis. During phosphodiester hydrolysis, negative charges are a common occurrence as the reaction proceeds. Nucleophiles become deprotonated and develop a negative charge or the attack of a nucleophile upon a phosphate causes the displacement of electrons onto the non-bridging oxygen atoms. Even the leaving group develops a negative charge upon being displaced from the RNA or DNA molecule. The introduction of a positively charged atom or compound can be used to great effect within this system since it can be used to direct negatively charged compounds or act as a Lewis acid.

Since metal ions develop positive charges in solution, metal ions are a prime candidate for use in phosphodiester hydrolysis. One does not even need to look between multiple nucleases to see the versatility of metal ions and permutations of catalytic mechanisms. In DNA polymerase I and Ribonuclease H, metal ions assist in the formation of a nucleophile, coordinate the nucleophile and stabilize the leaving group. (Beese 1991, Vivo 2008) Upon comparison between nucleases, the number of permutations only increases. Magnesium ions in RNase H stabilize the non-bridging oxygen atoms instead of a leaving group while alkaline phosphatase uses only zinc to coordinate the nucleophile. (Holtz 1999, Nowotny 2005) The number of variations and permutations available for metal ions within phosphodiester hydrolysis is the key reason for the widespread use in catalyzing phosphodiester hydrolysis. Positively charged metal ions complement the negative charges that develop and metal ions can be adapted easily for directing and coordinating negative molecules. Different permutations of metal ion catalysis are developed since differing environmental conditions within cells prompt for different strategies. In addition not all of these variations on metal ion catalysis

contribute equally with some forms of contributing greater or lesser amounts to the overall catalytic mechanism.

Catalytic Contribution to Catalysis

To better understand the contribution of metal ion catalysis within enzymes, research is often conducted by focusing on mutations. Amino acids that are suspected to be involved in a catalytic mechanism are substituted with others to negate all activity and deduce how much the mechanism contributes to catalysis. Mutations studies are often used in conjunction with structure studies like X-ray crystallography in order to pinpoint which residues could be involved in catalysis. For many of these enzymes, the loss of a metal ion causes the rate to plummet and in some cases fail completely. In I-PpoI, the asparagine 119 residue, which is hypothesized to coordinate with the Mg^{2+} ion, was mutated to alanine in order to eliminate the oxygen atom which was thought to coordinate with the Mg^{2+} ion. (Mannino 1999) This resulted in a 15,384-fold decrease in the rate of hydrolysis associated with the loss of coordinate with the Mg^{2+} . (Mannino 1999) Similarly in EcoRV, Asparagine 90 and 74 are thought to coordinate with divalent metal ions and upon mutation to alanine no catalytic activity is observed. (Imohof 2009) With the HDV ribozyme the Mg^{2+} is coordinated by both Guanine 25 and Uracil 20 and a double mutation to adenine and cytosine causes the rate to be equivalent to an HDV ribozyme with no Mg^{2+} bound. (Chen 2013) For all these studies, the loss in rate was associated with the loss of a bound metal ion. Since the residue needed to contact the metal ion was no longer present, the metal ion could not be bound. Enzymatic mutation studies are often used to assess the highest possible contribution a metal ion can make to

catalysis. The premise is that upon mutation of the involved residues, any interaction with the metal ion is completely lost and so the drop in rate can be associated with the metal ion. This methodology is used to assess the max contribution to catalysis because the complex nature of interactions within the enzymes means that replacement of an amino acid could also interrupt additional interactions and even the structure of the enzyme.

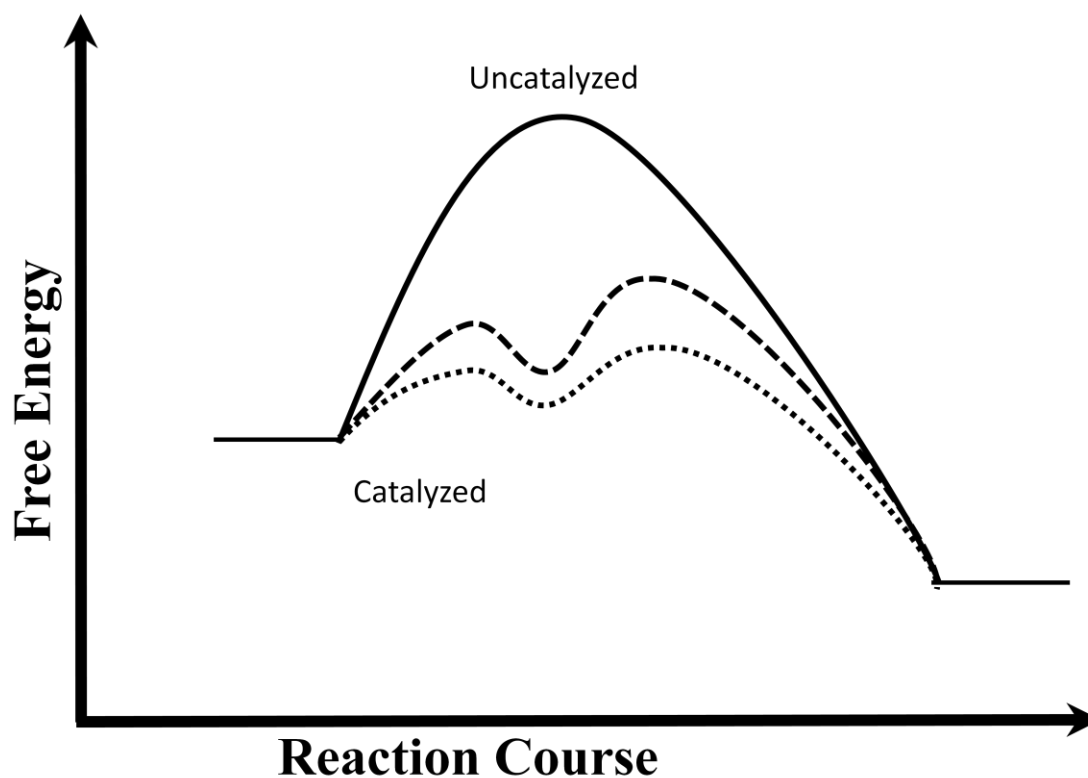


Figure 12: Catalytic mechanisms decrease the activation energy of a reaction resulting in an increase in rate since less energy is required to reach the transition state. As additional catalytic mechanisms are introduced activation energy is reduced further, indicated by the lower of the two dotted lines.

The complex web of interactions of amino acids within enzymes is one of the main drawbacks since one small change could have unforeseen effects within the enzyme and catalytic mechanism. The change in rate for mutation studies is considered the max

contribution as additional interactions or catalytic mechanisms can easily be interrupted and lead to an overestimation of contribution. Figure 12 highlights how additional interactions result in a further decrease in activation energy. In the HDV study, mutations had to be carefully selected to ensure minimal disruption to the ribozyme structure to see the contribution from only the metal ion. (Chen 2013) If the structure is unknowingly disrupted, a false positive of metal ion binding could occur or the amount of catalytic contribution could be overestimated. Also amino acids are not always confined to one form of catalysis. The asparagine in I-PpoI discussed previously can coordinate with Mg^{2+} but is thought to assist directly in catalysis by donating a proton to the scissile phosphate. (Mannino 1999) In this case the contribution to catalysis would be overestimated since two catalytic strategies would be altered instead of just the target mechanism. Complications such as these make mutation studies a good choice to determine the maximal contribution to catalysis and ways to approximate how much a mechanism can contribute to catalysis. Due to the possibility of interrupting intramolecular forces, structure and multiple catalytic mechanisms, many researchers have opted to using model systems to study enzymatic mechanisms.

Models systems are chemical systems that are made to emulate the forms of catalysis used by enzymes by using reactants that mimic the target molecules. (Rawlings 2006) These simplified systems are useful since individual catalytic strategies can be better isolated and experimental conditions can be more easily manipulated to see the effects on the system. Many studies vary the pH from acidic to alkaline or increase the temperature to levels above or below those found in biological systems in order to perturb the mechanisms. Depending on the sensitivity of the enzyme, the enzyme may denature

with relatively little change in pH or temperature which can put tight constraints on enzymatic experiments. Many researchers have opted for model systems in order to push the limits and see how these reactions can be perturbed under various conditions and to better elucidate the mechanisms.

Model Systems

Model systems using simplified DNA/RNA molecules have been used with great success so far to quantify the contribution of metal ions to phosphodiester hydrolysis. In order to develop a better picture of how catalysis can be affected, differing conditions and reactants are used to study metal ions from a variety of angles. A T5PNP DNA model system found that at 50°C and pH 7.8-8.5, Ca^{2+} could catalyze a reaction through a parallel single or double ion mechanism. (Kirk 2009) The mechanism was determined by fitting various mathematical equations to the data and selecting the one with the best fit. The mechanisms catalyzed the reaction 90 and 900-fold respectively with a contribution of 12kJ/mol for the first Ca^{2+} ion and 6kJ/mol for the second Ca^{2+} ion. (Kirk 2009) A similar experiment was conducted with Mg^{2+} and 1800-fold catalysis was observed with a one ion mechanism and an energy contribution of 20kJ/mol. Success has also been observed with RNA dinucleotide model systems such as Uridine monophosphate Uridine (UpU) which has been utilized with a variety of metal ions. (Ora 1998) Metal ions utilized include enzyme relevant ions, Zn^{2+} and Mg^{2+} , with a variety of others metal ions that are often used to determine the mechanisms of model systems: Mn^{2+} , Cd^{3+} and Gd^{3+} . (Ora 1998) At pH 5.6, Zn^{2+} and Mg^{2+} had a 139 fold increase in rate and a 2 times increase respectively. Mn^{2+} , Gd^{3+} and Cd^{3+} had increases of 12.5, 19000 and 38

respectively. (Ora 1998) Comparisons between studies that look at the contribution of metal ions can be useful in determining what environments limit catalysis or contribute to maximizing catalysis. For example, when comparing the previous studies, one can see that Mg^{2+} provides less catalysis in an acidic environment compared to a more basic environment. Information pertaining to when catalysis occurs is useful to researchers since different metal ion or reactants can be used to form different models to simulate different situations.

Recently many model systems have emphasized maximizing catalysis and determining what metal ions and metal ion complexes can be used to maximize catalysis in an attempt to make artificial enzymes competitive with natural nucleases. These systems tend to focus on using transition metals, lanthanide metals and complexes containing these metals in order to maximize catalysis. (Rawlings 2006) Most of these metal ion systems are conducted in acidic or neutral pH since many metal ions and metal complexes become increasingly insoluble and so precipitate easily in alkaline pH's. Thus these metals cannot be present in sufficient concentrations. This has resulted in the metal catalyzed reaction in an acidic environment being relatively well studied while research conducted in a basic environment has received much less focus. Metal ions that can dissolve to sizable amounts in basic environments, like Ca^{2+} , are not known for being catalytic powerhouses and so little research has been pursued since other metal ions could be adapted easier to an efficient artificial enzyme.

Understanding the how of metal ion catalysis is also important when studying model systems. Knowing how much a metal ion can contribute to catalysis is useful but being able to associate a mechanism and transition state with the contribution is what

allows researchers to have the full picture. As previously discussed, KIEs can be useful for elucidating transition states that occur when the general mechanism is known. (Ora 2011) In order to develop a clearer idea of the catalytic mechanism the metal ion is participating in, many researchers utilize thiosubstitution. (Zhao 2002) Thiosubstitution is when a sulfur atom is substituted in the place of another atom of a reactant molecule, illustrated in Figure 13. (Ora 1998) Most metals have varying affinities for oxygen and sulfur, with some having a preference for one or even neither. If the metal ion in question has a difference in affinity between oxygen and sulfur, a thiosubstituted molecule is used to see if there is a change in the binding of the metal ion based on the thio effect. (Liang 2010, Zhao 2002) The thio effect is an indication of the change in the rate constant due to a difference in binding to the target molecule. The thio effect is reported as k_o/k_s , where k_o is the rate constant of the non-thiosubstituted molecule and k_s is the rate constant of the thiosubstituted molecule. (Purcell 2005)

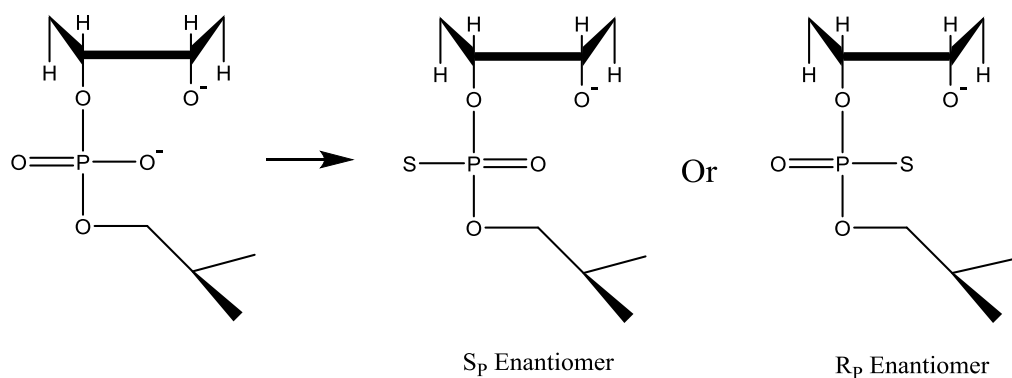


Figure 13: Example of a thiosubstitution on a generic RNA molecule. A thiosubstituted molecule is one in which a specific atom is chosen and exchanged for a sulfur atom. In this example, a non-bridging oxygen atom was selected and exchanged for a sulfur atom in the other molecule. The substitution of a non-bridging oxygen atom around the phosphorus results in two chiral products denoted by R_P, R-chirality around the phosphorus, or S_P, S-chirality around the phosphorus.

Thio-substitution has been utilized in enzyme studies in order to determine the role of metal ions within a reaction such as with PI-PLCs, an enzymatic protein involved in phosphoryl transfer. (Ora 1997, Zhao 2002) This methodology was utilized in order to determine which non-bridging oxygen coordinated with Ca^{2+} in order to facilitate catalysis. Ca^{2+} has a higher affinity for oxygen than sulfur therefore when a thiosubstitution is performed a decrease in binding should be observed. (Zhao 2002) So by determining which stereoisomer incurred a rate deficit the researchers were able to identify which non-bridging oxygen atom Ca^{2+} was interacting with. Thiosubstitution studies have also recently been applied to studying the effects of metal ions with model systems. Researchers used a thiophosphate of adenosine 5'-O-monophosphate (AMP) to determine how the introduction of a sulfur molecule influenced the stability of the metal-AMP complex. (Sigel 1997) It was determined that soft metal ions, such as Cd^{2+} and Zn^{2+} , which typically have an affinity for sulfur, had greater stability with the thiophosphate model. However, harder metal ions, such as Mg^{2+} and Ca^{2+} which bind stronger to oxygen, had no difference in binding. (Sigel 1997) Alternately some researchers using model systems instead monitor how the rate constants change upon the introduction of a sulfur molecule. (Ora 1997) This work follows a similar vein to the enzyme studies where increases and decreases in rate indicate where the metal ion of interest is binding based on where the substitution occurs. Although in some situations, as observed in the Sigel 1997 study, the results can vary from model to model. Ca^{2+} typically shows less binding to sulfur and other softer atoms, yet in the Sigel 1997, no increase or decrease was observed. Thiosubstitution is a useful technique but it is not the

solution to all model systems. This is why combinations of techniques are used in conjunction to identify locations of metal binding and possible mechanisms of catalysis.

Although understanding the mechanism and contribution to metal catalysis is important, the knowledge can be used to great effect in other areas. Knowing how natural nucleases work and what conditions promote effective catalysis is important to designing small molecules that mimic natural nucleases. Application of this knowledge has already been used to great effect in designing a variety of artificial nucleases based on naturally occurring enzymes. (Feng 2006)

Emulation of Natural Nucleases: Artificial Nucleases

There are a myriad number of naturally occurring nucleases that are currently used but the application of synthetic peptidases and nucleases could have a significant impact for both medical and research applications. (Hegg 1999, Feng 2006) One of the biggest applications of a synthetic nuclease is for use as an artificial restriction enzyme. For biologists that need to target a specific sequence but lack a natural enzyme for that specific sequence, an artificial restriction enzyme would be of monumental importance. (Hegg 1999, Feng 2006) Currently there is a large library of natural nucleases that can be selected for genetic modification, yet artificial nucleases can further increase the size of the library. Also, if the specificity and efficiency of artificial nucleases reaches a preferred level, there is even the possibility of incorporating artificial nucleases as therapeutics. (Murtola 2008) This is an objective of those in the antisense field where the precise destruction of mRNA *in vivo* with artificial nucleases could be a viable way to treat medical conditions associated with the over expression of proteins. (Hall 1996) The

antisense field covers individuals involved in the production of pharmaceuticals which bind to a target mRNA molecule and provide a therapeutic effect.

Research into naturally occurring forms of phosphodiester cleavage can yield information that can be useful for the production of synthetic nucleases. Using natural enzymes as models for enzymatic catalysis can yield information on enzyme substrate specificity or metal ion catalysis of phosphodiester models can yield activation parameters and mechanisms that can be applied to synthetic nucleases. (Lonnberg 2011) Current research into artificial nucleases is proceeding through two different paths: specificity and enzyme efficiency. Research into transcription activator-like effector nucleases (TALENs) and zinc-finger proteins are focused primarily on increasing the specificity of nucleases, as illustrated in Figure 14. (Beurdeley 2012) These motifs are being designed to target specific sequences of DNA or RNA to allow pinpoint targeting of sequences. Even if a small molecule is produced that can rival the efficiency of a natural nuclease, it will have little use if it cleaves any phosphodiester that gets near it.

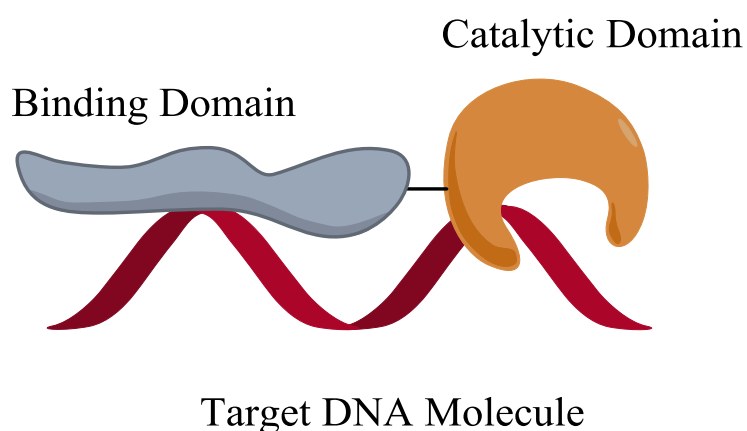


Figure 14: Simple pictorial representation of an artificial nuclease. This diagram consists of a binding domain, such as a TALEN, which binds to the target DNA or RNA molecule. In addition a catalytic domain, such as a metal complex, attached to a binding domain will catalyze a phosphodiester bond cleavage.

The other path, enzyme efficiency, is focused on maximizing the cleavage ability through a number of catalytic strategies based on natural nucleases and metal ion catalysis. (Whitney 2002, Putnam 2001, Hall 1996) Some studies focus primarily on the cleavage part of the molecule such as in the Feng 2006 study. The objective of this study was to increase the cleaving efficiency of a complex that used two zinc ions to induce catalysis. (Feng 2006) Each zinc ion acted as a Lewis acid and stabilized the transition state of the phosphate complex. (Figure 15) Since seeing that their original complex could induce cleavage at significant rates, the researchers have begun to explore how their model could be further adapted to rival the rates seen in biological enzymes. (Feng 2006) Yet other researchers attempt to combine both paths together in an attempt to see how effective the sum of the techniques can be. In the Putnam 2001 study, researchers made a ribozyme mimic by combining a known RNA hydrolysis cleaving agent that contained a copper ion to a strand of DNA that was 17 base pairs long that acted as the specificity component. Some changes were made to the structure of the cleaving agent in an attempt to maximize efficiency and they found that some of their changes to the cleaving agent had up to a 10-fold increase in the rate of cleavage. (Putnam 2001) All work that is done to produce artificial nucleases is incremental with changes being made and tested to see what improves different functions of the nuclease. Little by little changes are made to various parts of the nucleases in an attempt to fine-tune and improve these nucleases in the hopes that one day they will rival natural nucleases. Some researchers have also begun to look into peptide nucleic acids or PNAs which are reported to be the first peptide nucleic acid based artificial RNA-cleaving enzymes. (Murtola 2008) PNAs act in a fashion similar to the ribozyme mimics except

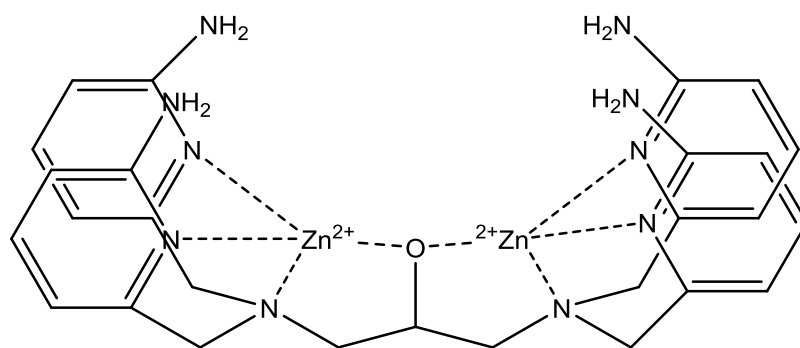


Figure 15: Metal complex developed in the Feng 2006 study which can act as a small molecular cleaving agent. Catalysis is induced by the Zn^{2+} ion acting as a Lewis acid and providing electrostatic stabilization to the non-bridging oxygen atoms. Additional NH bonds were added in order to give some specificity to the molecule.

PNAs do not have a nucleic acid based backbone. Instead a backbone consisting of a peptide bond, a link between a carboxyl group and an amino group, is used. (Murtola 2008) PNA based systems are said to form more stable complexes with complement DNA or RNA strands and are stable within biological environments. A PNA-based system using a metal-cleaving head was first produced successfully in 2002. (Whitney 2002) This specific system was able to cleave an 11 nucleotide sequence successfully with a cleaving head containing a zinc ion. (Whitney 2002) In the same vein of experiments, another study developed a PNA that could successfully cleave an RNA sequence that was related to leukemia in the presence of zinc. (Murtola 2008) The rate of cleavage was less than satisfactory for suppressing the gene expression but this study showed that PNA based nucleases contain a number of properties necessary for an artificial nuclease. (Murtola 2008) A vast amount of research has been poured into these systems due to the potential effects in the scientific and medical fields. Similar to how the first nucleases evolved within organisms, each adjustment to artificial nucleases brings researchers closer to achieving their goal. In order to develop better cleaving

small molecules, it is essential to develop a variety of model systems to model various situations and possible catalytic situations.

Current Research

Open Questions

Although phosphodiester model systems have been researched thoroughly over the years there are still gaps in the literature. One of these gaps was mentioned previously and that is the characterization of metal catalyzed phosphodiester hydrolysis at a highly basic pH. There has been a copious amount of studies focused on neutral and acidic reactions such as the Mikkola 1999 study which used the buffers MES (pKa 6.15) and HEPES (pKa 7.0). When experiments have been conducted at basic pH's there has been no metal catalyst present or the pH's were only slightly basic. The Harris 2010 study looked at just phosphodiester hydrolysis at pH's 12 and 14 while the Rawlings 2006 study looked at pH's around 8.5 when using various transition and lanthanide metals. The lack of research in this area is mostly due to the various metals and metal complexes already having relatively low solubility and even lower at a heightened pH. (Bruice 1996) So the development of a metal-catalyzed phosphodiester RNA model that could function at higher pH's would be able to help unravel questions regarding the basic metal-catalyzed phosphodiester hydrolysis of RNA.

This directly leads to the next set of questions, how does the mechanism of metal catalysis differ at basic pH's compared to acidic pH's? Several models have been developed for both DNA and RNA and have determined that two different forms of catalysis are possible. Studies such as the Mikkola 1999 study have observed that

general acid catalysis is a viable form of metal ion catalysis. Various alkyl leaving groups were used in order to investigate the sensitivity to reactivity of the leaving group. Addition of Zn^{2+} resulted in alkyl substrates that appeared less sensitive to pH, indicating that Zn^{2+} may be involved in general acid catalysis. (Mikkola 1999) Yet there is research indicating that association with the non-bridging oxygen atoms is entirely possible through interaction as a Lewis acid. (Browne 1992, Sigel 1996, Korhonen 2011) This form of catalysis was determined to be the form of catalysis in the Korhonen 2011 study in which various types of alkyl esters were subject to varying conditions. It was observed that the B_{LG} values of the Zn^{2+} catalyzed alkyl phosphoesters were similar to those of a nucleoside 3' phosphotriester under neutral conditions. It was concluded that the mechanisms are similar and so the Zn^{2+} catalyzed reaction must proceed with the Zn^{2+} neutralizing the charge on the phosphate and stabilizing the formation of the phosphorane.

Identification between multiple mechanisms can prove to be problematic depending on the substrates chosen. KIE's can be used to discern if general acid or general base catalysis is occurring, but it is entirely possible that this method will tell you that neither is occurring if proton transfer is not part of the catalytic mechanism. Usage of a thio-substituted molecule to determine how a metal ion is associating with the substrate is another possibility. Yet some of the more popular metal ions such as Zn^{2+} do not have widely differing affinities for sulfur and oxygen which complicates identifying how these metals interact with the model. Is it possible to make a model system that not only catalyzes RNA phosphodiester hydrolysis at basic pH's but that also allows for the elucidation of what mechanism is at play?

Current Study

The current study aims to test the validity of a model for metal-catalyzed phosphodiester hydrolysis in a basic environment. To that end, we have chosen Ca^{2+} as our metal ion of choice since Ca^{2+} , compared to other metal ions, has a relatively high solubility in a basic environment in addition to inducing respectable increases in reaction rate. The RNA model chosen was Uridine monophosphate Gaunosine, UpG, a simple dinucleotide model. The reason why Ca^{2+} has had only minor research compared to other metal ions is due to its modest catalysis of phosphodiester systems at neutral and acidic conditions. Even at higher concentrations of Ca^{2+} , the catalytic potential is far less than transition metals ions and lanthanide ions which have greater catalysis potential at lower concentrations. An additional benefit of this model is that only cleavage occurs with no pseudorotation or isomerization occurring since it is in a basic environment where the phosphorane intermediate is not stable enough for additional reactions to occur. This

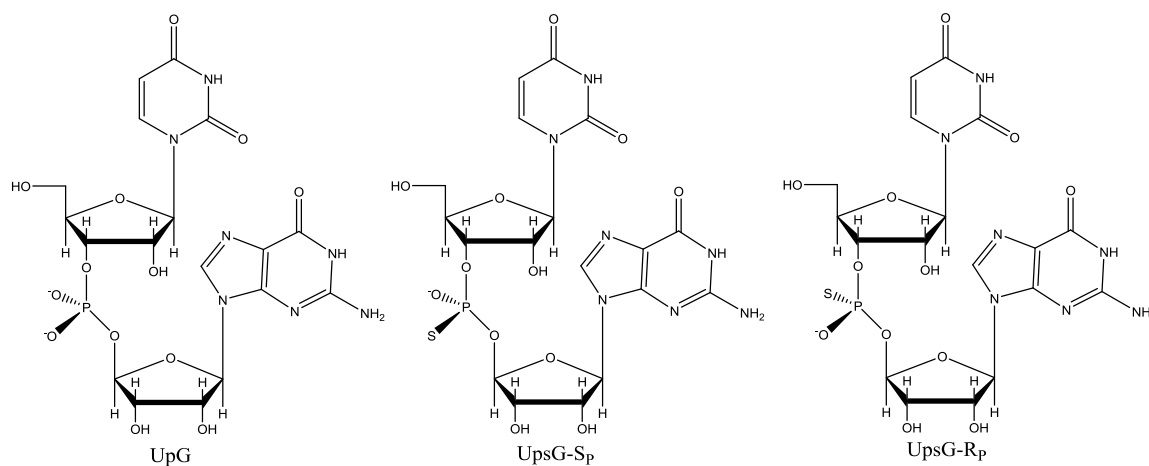


Figure 16: Uridine monophosphate Gaunosine (UpG) and the thio-substituted versions of UpG, Uridine monophosphorothioate Gaunosine (UpsG). The thio-substituted model exists as two stereoisomers denoted by their chirality around the phosphorus. S_P denotes S chirality around the phosphorus and R_P denotes R chirality around the phosphorus.

means that any changes made to the system should only affect the cleavage of the RNA model allowing researchers to more easily visualize and identify the effects of manipulated conditions with phosphodiester hydrolysis.

After observing that Ca^{2+} did have a catalytic effect on the phosphodiester hydrolysis of our RNA model Uridine monophosphate Guanosine (UpG, Figure 16), solvent deuterium isotope effects (SDIE) were utilized in an attempt to discern if Ca^{2+} catalysis involved general acid or general base catalysis. To our surprise, the SDIE's indicated neither general acid nor general base catalysis. We then suspected that Ca^{2+} was instead associating with the non-bridging oxygen atoms and providing electrostatic stabilization to the phosphorane intermediate, Figure 10. This prompted the use of a thiosubstituted model since Ca^{2+} does show varying affinities for hard Lewis bases like oxygen and softer Lewis bases like sulfur. The thiosubstituted RNA model had two stereoisomers identified as R_P , R-chirality around the phosphorus, and S_P , S-chirality around the phosphorus, both of which showed slight rate deficits. Further research will be conducted using a dithiosubstituted model where both oxygen atoms have been replaced by sulfur to confirm if Ca^{2+} can still cause catalysis with only one oxygen atom present.

Materials and Methods

Reaction Kinetics

Uridine-monophosphate Gaunine, UpG, (Dharmacon) stock solutions were deprotected according to instructions from Dharmacon. Following resuspension, concentrations of the original stock solution were determined based on Beer's Law using an ϵ_{260} of $20000 \text{ M}^{-1}\text{cm}^{-1}$ using a Beckmann 630 DU spectrophotometer. Aliquots containing 5 nmoles of UpG were dried using a Speed Vac SC110 and stored at -20°C until reaction initiation.

UpsG stock solutions were deprotected as above. R_P and S_P enantiomers were separated and isolated using an Agilent 1100 Series HPLC with a Phenomenex C18 300X390 mm 10 micron column and eluted isocratically using a mobile phase consisting of 3% acetonitrile, 0.1M ammonium acetate in water. Stock solutions were dried using a Speed Vac SC110 and resuspended in 1 mL of double deionized water.

This process was repeated an additional four times to remove the ammonium acetate salt. The isolated stock solutions were then resuspended in one microcentrifuge tube and spun down in a Desktop Microcentrifuge Eppendorf 5424 at 15,000RPM for 15 minutes. The supernatant containing the UpsG was collected and the concentration was determined based on Beer's Law using an ϵ_{260} of $21500 \text{ M}^{-1}\text{cm}^{-1}$. Aliquots containing 2 nmoles were dried using a Speed Vac SC110 and stored at -20°C until reaction initiation.

The initiation mixture for thio effect studies consisted of a 500 μL solution containing 50mM of pH 11.5 CAPS buffer (Sigma Aldrich) and 0-0.33M CaCl_2 (Sigma Aldrich) with ionic strength maintained at 1.00 with NaCl (Sigma Aldrich). Experiments were conducted at 37°C . Reactions were quenched at indicated time points by 50 μL of 87.5mM EPPS free acid (Sigma Aldrich) to pH 7-8. The samples were then stored at

-20°C until HPLC analysis. Experiments used to determine the order of the reaction consisted of 0.33 M CaCl₂ and 50mM CAPS buffer from pH 10.8 to 11.5. Mock solutions were made to determine the actual pH of the reaction mixes.

For solvent deuterium isotope effect studies, separate stock solutions for CaCl₂ and NaCl were made with D₂O (Sigma Aldrich) as the solvent. The initiation mixture for this part of the study consisted of 500 µL of 0.33 M CaCl₂ and 3.3 mM NaOH for a pH of 11.5. Reactions were quenched at indicated time points by 45 µL of 50 mM EPPS free acid to pH 7-8. Samples were stored at -20°C until HPLC analysis.

HPLC Analysis of Reactions

During the course of the experiment, a separation technique known as HPLC was utilized to separate a variety of compounds for collection and analysis purposes. HPLC consists of two phases, a mobile phase and a stationary phase, the composition of which can vary with the analytes of interest. The mobile phase is a liquid medium that is high in purity and is a solution consisting of two liquids. The mobile phase is pushed at a high pressure through the system by a pump and is used to carry the analytes through the system to a detector. The analytes are injected into the system and are carried by the solvent to the stationary phase of the HPLC which is located in the column. In most systems the stationary phase consists of pure, spherical, microporous particles of silica which have a very high surface area and allow solvent to pass through. The silica can be modified to change the properties of the stationary phase. This current work uses a stationary phase modified with C₁₈ groups to make the stationary phase more hydrophobic.

The separation of analytes occurs within the column and is influenced by the composition of both the mobile phase and stationary phase. The rate by which an analyte passes through a system is determined by how well solvent molecules adsorb to the stationary phase compared to the analyte molecules. The better the analyte molecules are able to compete for adsorption sites on the stationary phase, the slower the analyte will move through the column. Thus the analyte will have a larger elution time, the time it takes to pass through the column. The composition of the mobile phase and the stationary phase can alter the elution time of the substances and can be altered to increase the resolution between analytes. In this current work with a hydrophobic stationary phase, analyte molecules with more hydrophobic groups will have longer retention times. The elution times for all analytes will be decreased upon increasing the concentration of the non-polar portion of the mobile phase by adding acetonitrile.

Finally after passing through the column, the substances pass through a detector to determine when the substances made it through the column. A number of detectors can be utilized and some such as the use of a photodiode array, as used in this work.

All samples were analyzed using reversed-phase chromatography. UpG aliquots were analyzed by Agilent 1100 Series HPLC with a water/acetonitrile mobile phase consisting of 3% acetonitrile and 0.1 M ammonium acetate and passed isocratically at 1.0 mL/minute through a Phenomenex C18 300X390 mm 10 micron column. UpsG-R_P aliquots were analyzed with a water/acetonitrile mobile phase consisting of 3% acetonitrile and 0.1 M ammonium acetate and passed isocratically through a Phenomenex C18 300X390 mm 10 micron column. An Xbridge C18 3.5 micron 4.6 X150 mm column was used for later trials with a flow rate at 0.5mL/minute. The UpsG-S_P aliquots

were analyzed with a water/acetonitrile mobile phase consisting of 4% acetonitrile and 0.1M ammonium acetate and passed isocratically through a Phenomenex C18 300X390 mm 10 micron column. An Xbridge C18 3.5 micron 4.6 X150mm column was used for later trials with a flow rate at 0.5mL/minute. The Phenomenex C18 300X390 mm 10 micron column was replaced for the UpsG-Rp and UpsG-Sp later trials due to column degradation. Due to column degradation, the peaks began to widen and eventually split into two separate peaks. This was considered unacceptable and the Xbridge C18 3.5 micron 4.6 X150mm column was chosen as the best from the available columns due to retention time and peak shape. The UpG and Guanine standards were run to determine elution time. (Cassano, Personal Communication)

Each peak was integrated manually using the HPLC software to quantify the absorbance at 260 nm. Peaks were integrated from when the far side of the peak reached baseline and a line was drawn straight across until the opposite side reached baseline. If overlap between two peaks occurred, each peak was measured the same except that the line was started opposite the overlap and drawn to where the center of the overlap occurred. The absorbance of each product was normalized by dividing by the extinction coefficient of the compound. The extinction coefficient for G was found to be $13,200 \text{ M}^{-1}\text{cm}^{-1}$ from the NIST Chemistry Webbook and $20,000 \text{ M}^{-1}\text{cm}^{-1}$ for UpG from the Ambion Oligo eta calculator. The UpsG R_p and S_p extinction coefficients were determined to be $21500 \text{ M}^{-1}\text{cm}^{-1}$ from the Ambion Oligo calculator.

Kinetic Analysis

The value proportional to concentration was then converted to fraction of UpG remaining by using Equation 1 or fraction of UpsG remaining using Equation 2.

$$fUpG = \frac{[UpG]}{[UpG] + [G]} \quad \text{Equation 1}$$

$$fUpsG = \frac{[UpsG]}{[UpsG] + [G]} \quad \text{Equation 2}$$

Where fUpG or fUpsG is the fraction of reactant remaining, [UpG] is the concentration of UpG in the aliquot, [UpsG] is the concentration of UpsG in the aliquot, and [G] is the concentration of the guanine product in the aliquot.

The rate constant of a reaction was determined by graphing the fraction of reactant remaining, fUpG or fUpsG, against time and fitting it to single exponential decay using Kaleidagraph™. The k_{obs} values that were obtained from the exponential decay were then plotted against concentration and fit to a rectangular hyperbola. (Equation 3)

$$k_{obs} = \frac{k_{max} * [Ca^{+2}]}{K_D + [Ca^{+2}]} + k_0 \quad \text{Equation 3}$$

Where k_0 is the rate where the $[Ca^{2+}] = 0$, k_{max} is the saturating rate constant for Ca^{2+} and K_D is the equilibrium dissociation constant for the $Ca^{2+} * UpG$ complex.

To determine the order of the reaction the $\log(k)$ was graphed against pH and fit to a linear regression for trials which contained the initiation mixtures with varying pHs. The slope was then used to determine the order of the reaction. For the solvent deuterium isotope effect studies, the kinetic isotope effect was determined with Equation 4.

$$KIE = \frac{k_{H_2O}}{k_{D_2O}} \quad \text{Equation 4}$$

Where k_{H_2O} is the rate constant in H_2O and k_{D_2O} as the rate constant in D_2O . Similarly the thio effect for the thio-substitution studies was determined by Equation 5.

$$\text{Thio}E = \frac{k_o}{k_s} \quad \text{Equation 5}$$

Where k_o is equal to the rate constant of the non-thiosubstituted model and k_s is equal to the rate of the thiosubstituted model. The energetic contribution to each the reactions were quantified using the Arrhenius Equation based on the difference on rate constant, Equation 6.

$$\ln(k_2) - \ln(k_1) = \frac{\Delta G}{RT} \quad \text{Equation 6}$$

Where k_2 is equal to the catalyzed rate constant, k_1 is equal to the uncatalyzed rate constant, R is equal to the gas constant and T is equal to the temperature of the reaction in Kelvin. Both rate constants were determined experimentally.

Results

HPLC analysis was able to successfully separate the guanosine (G) product from both the UpG, UpsG-S_P and UpsG-R_P reactants. (Figure 17) For UpG reactions analysis, the product G peak has a retention time of approximately 6.3 minutes and the UpG has a retention time of approximately 7.9 minutes. For UpsG-R_P reaction analysis, the product G peak has a retention time of approximately 11 minutes and the UpsG-R_P has a retention time of approximately 22 minutes. For UpsG-S_P reaction analysis, the product G peak has a retention time of approximately 6 minutes and the UpsG-S_P peak has a retention time of about 25 minutes. The size of the UpG and UpsG peaks decreased at later time points while the size of the G peak increased at later time points. (Figure 17) This is indicative that RNA phosphodiester cleavage is occurring. As seen in Figure 17, tailing of the product peak for UpG samples occurred at later time points with some overlap of the reactant and product peaks. Once the data was quantified, it appeared that there was little to no interference with the measurements due to the high accuracy of the exponential decay fits. Similarly for the UpsG-S_P and R_P stereoisomers, fronting peaks occurred but with no overlapping of product and reactant peaks.

The data can be quantified using the HPLC software to manually integrate individual peaks. From Beer's Law and Equation 1, the fraction of UpG remaining can be determined to calculate the rate of each reaction. To determine the rate of a reaction, the fraction of UpG remaining of an aliquot is graphed against time and fit to single exponential decay using KaleidagraphTM. If Ca²⁺ does catalyze phosphodiester hydrolysis of RNA, an increase in rate should be observed as Ca²⁺ concentration is increased. Figure 18 depicts the increase in rate constant as the concentration of Ca²⁺

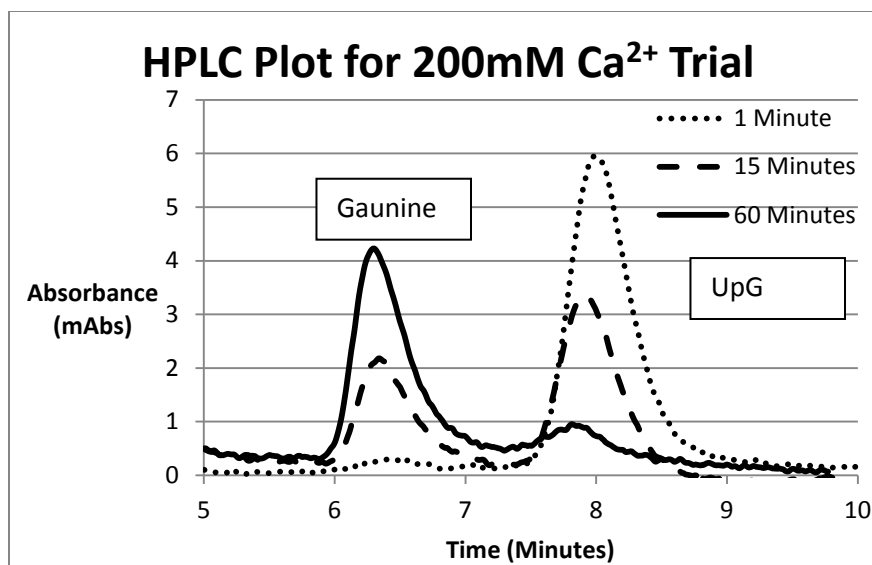


Figure 17: HPLC Data of a neutralized 200mM Ca²⁺ trial at 37°C at pH 11.5 and ionic strength of 1. Aliquots from 1 minute, 15 minutes and 60 minutes are shown. UpG reactant's retention time is about 7.9 minutes and G product peak has a retention time of about 6.3 minutes. As the reaction proceeds, the amount of reactant decreases and the amount of product increases. The peak area is proportional to the concentration of compound.

increase. At 0.10 M Ca²⁺ a k_{obs} of 0.023 is calculated, 0.20 M Ca²⁺ yielded a k_{obs} of 0.040 and 0.33 M a k_{obs} of 0.054 was calculated. The correlation between increasing Ca²⁺ concentration and rate constants is consistent with Ca²⁺ catalyzing the reaction. Examining the k_{obs} , as a function of the Ca²⁺ concentration can provide information regarding the mechanism of catalysis.

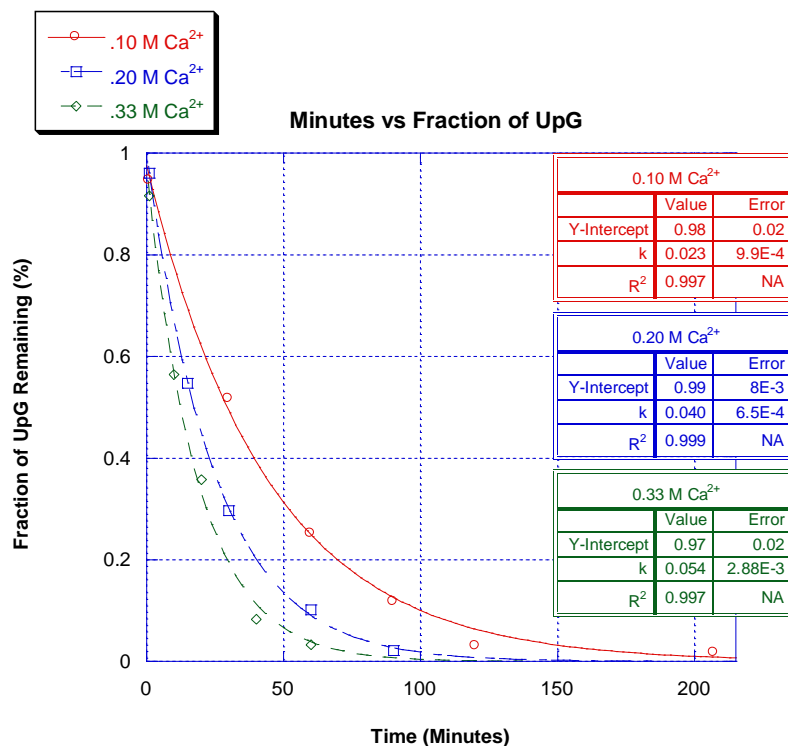


Figure 18: Fraction of UpG remaining against time elapsed in neutralized 60 μ L aliquot containing 0.10 M (red circles), 0.20 M (blue squares) or 0.33 M Ca²⁺ (green diamonds) at pH 11.5 and 37°C with a ionic strength of 1. The fUpG was determined by HPLC analysis and associated calculations as outlined in the Methods section. Each line is fit to an exponential fit and represents a different concentration trial. As the concentration of Ca²⁺ increases, there is also a corresponding increase in the rate of the reaction.

The k_{obs} vs Ca²⁺ data were fit to a rectangular hyperbola model (Figure 17) with an R² value of 0.985. (Figure 19) A linear fit was also applied which resulted in a R² value of 0.970. The rectangular hyperbola model was determined to be the more accurate model due to a higher R² value. The rectangular hyperbola model suggests saturation at high Ca²⁺ concentrations with a maximum rate constant, k_{max} . The k_{max} value was determined to be 0.170, a 326-fold increase when compared to the noncatalyzed rate constant. This results in an energetic contribution of 14.9KJ/mole. The lack of upward

curvature indicates that multiple Ca^{2+} ions are not involved in the mechanism of catalysis and only one Ca^{2+} ion is involved in catalysis. (Kirk 2010)

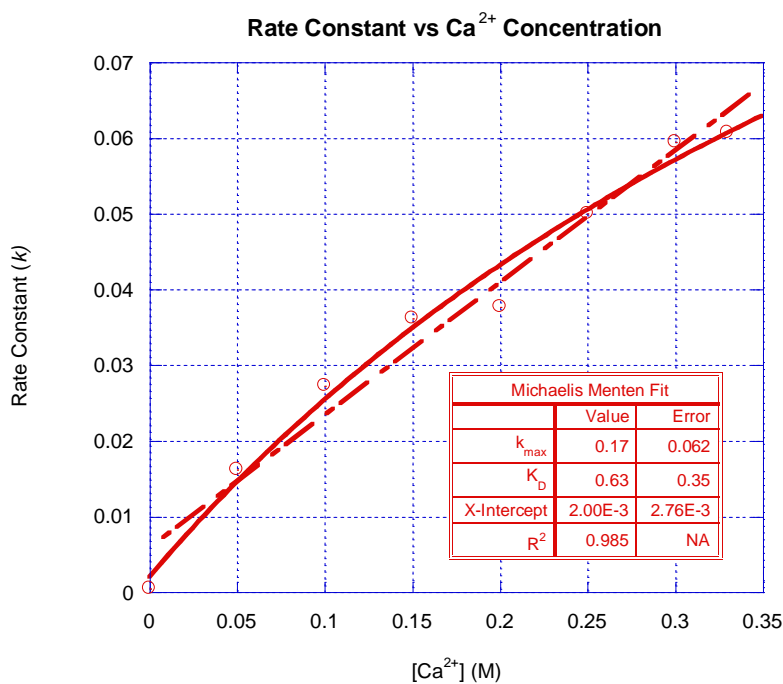


Figure 19: Plot of average rate constant, determined from the exponential fit of fraction of UpG remaining against time, against the concentration of Ca^{2+} . All trials were conducted at pH 11.5, 37°C and at an ionic strength of 1. All points are the average rate determined over 3 trials with error bars are representative of the standard deviation of each set of points. This plot is fit to a rectangular hyperbola (solid line) which means that RNA Ca^{2+} catalysis most likely proceeds by a different mechanism from DNA Ca^{2+} catalysis. Linear fit is also included as dotted line.

In order to confirm the order of the reaction with respect to hydroxide, the pH was varied while the CaCl_2 concentration was kept constant. The results were graphed as the $\log(k)$ vs pH which resulted in a linear graph with a slope of approximately 1 which is indicative of a 1st order reaction. (Figure 20) (Dahm 1993) This data is from 1 set of trials and more trials would be beneficial to confirm that the reaction is first order. However, it

is consistent with previous research on alkaline cleavage of RNA and metal catalyzed RNA cleavage. (Ovianen 1995)

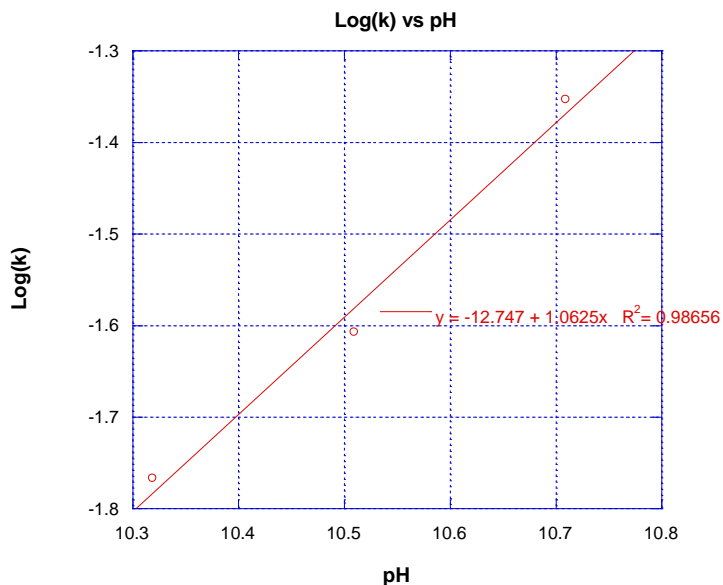


Figure 20: This graph was produced by using initiation mixtures that contained a constant .33M CaCl_2 with CAPS buffer at pHs 10.8-11.5. The pH Mock initiation mixtures were determined to yield the actual pH of the reaction. This graph is representative of one data set and gives a slope of around 1.06. This is indicative of a 1st order reaction with respect to hydroxide.

The k_{obs} vs Ca^{2+} data for the thio-substituted models were fit to a rectangular hyperbola model. (Figure 21) The R^2 value for UpsG-S_P was found to be 0.97 and for UpsG-R_P it was 0.97. A linear fit was applied to UpsG S_P and UpsG R_P resulting in a R^2 value of 0.94 and 0.96. The rectangular hyperbola model appears to be the more accurate model due to a higher R^2 value and allows direct comparison with UpG. Table 1 was produced based on Figure 21 and includes the k_{max} , K_D and rate enhancement of the non-catalyzed reaction of UpG and both stereoisomers of UpsG. The rate enhancement of UpG compared to the uncatalyzed reaction was equal to 326-fold faster, for UpsG-S_P the

rate enhancement was 81-times faster and for UpsG-R_P the rate enhancement was 106-fold faster. The corresponding energetic contributions were, respectively, 14.9KJ/mol, 11.3KJ/mol, and 12.0KJ/mol and calculated based on Equation 6. Finally the K_D of the UpsG-R_P was found to be about the same as that of the UpG model and the K_D of the UpsG-S_P was half that of the UpG model. The large error value associated with the UpsG-R_P K_D value is most likely due to the lack of significant curvature at higher concentrations of Ca²⁺. The K_D values were used to calculate the ΔG for all trials. The ΔG for UpG was determined to be -1190 J/mol, the ΔG for UpsG-S_P was determined to be -4020 J/mole and for UpsG-R_P the ΔG was determined to be -271 J/mol. The ΔΔG comparing UpG to UpsG-SP was calculated to be 2830 J/mol and the ΔΔG comparing UpG to UpsG-RP was calculated to be -919 J/mol. The little change in affinity and the small change in k_{max} values indicates that little to no thio effect has occurred with the thio-substituted models. All data presented here is shown in Table 1.

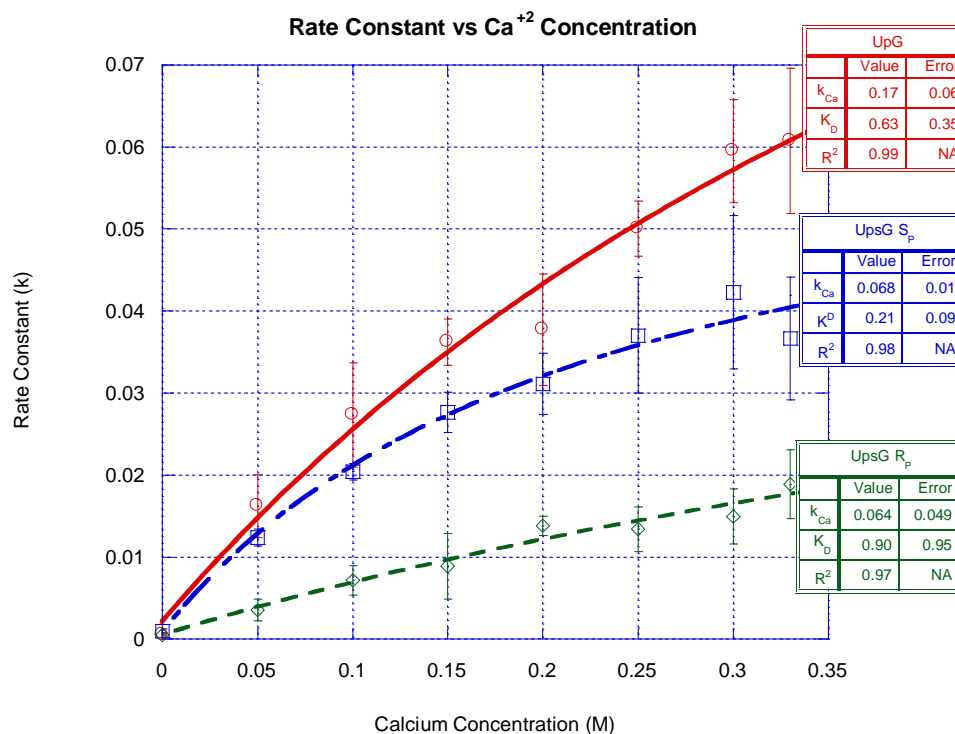


Figure 21: Plot of average rate constant, determined from the exponential fit of fraction of UpG (red), UpsG-R_P(blue) and UpsG-S_P (green) remaining against time, against the concentration of Ca²⁺. All trials were conducted at pH 11.5, 37°C and at an ionic strength of 1. All points are the average rate determined over 3 trials with error bars are representative of the standard deviation of each set of points. This plot is fit to a rectangular hyperbola to determine the k_{max} and K_D of all substrates and only a small thio effect is observed between substrates. Linear fit of UpsG-S_P, blue dotted line, and R_P, green dotted line overlapping with rectangular hyperbola fit.

Table 1: Rectangular Hyperbola Fit Data Summary								
	k_{max}	Error	K_D	Error	k_{max}/k_D	$^\ddagger G$ (KJ/mol)	ΔG (J/mol)	$\Delta\Delta G$ (J/mol)
UpG	0.17	0.06	0.63	0.35	326	14.9	-1190	0
UpsG S_p	0.068	0.01	0.21	0.09	68	10.9	-4020	2830
UpsG R_p	0.064	0.049	0.9	0.95	129	12.5	-271	-919

Thio effects were calculated individually for each concentration of CaCl_2 and for each stereoisomer. (Figure 22) The average thio effect ratio for the R_P stereoisomer was calculated to be 3.73 ± 0.56 and for S_P it was calculated to be 1.37 ± 0.13 indicating the lack of a significant thio effect. The lack of a clear upward trend in thio effect for either enantiomers also indicates that the presence of a sulfur atom did not hinder catalysis by Ca^{2+} .

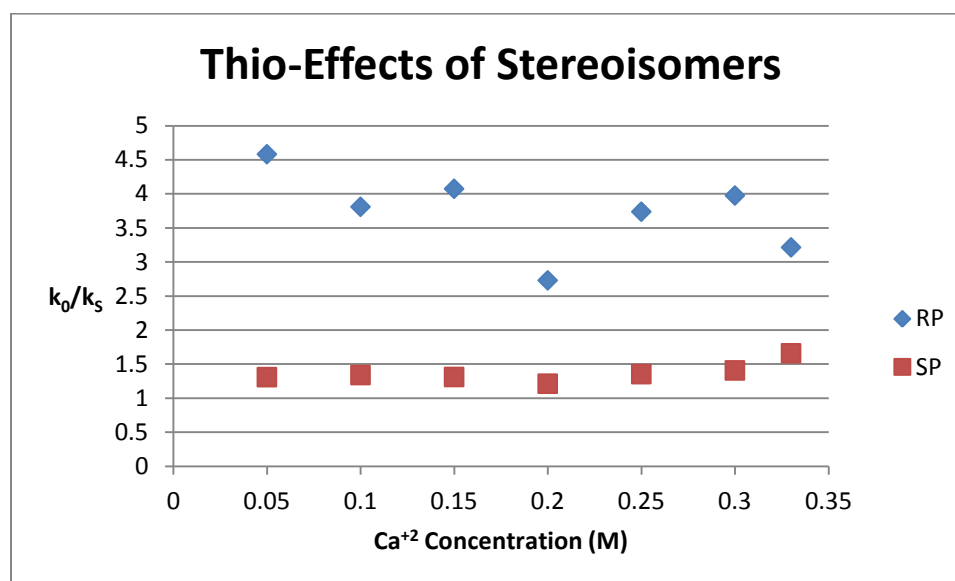


Figure 22: Graphical representation of the difference in rate between the non-thiosubstituted UpG and both stereoisomers of the thiosubstituted UpG, UpsG R_P (blue) and UpsG S_P (red). Thio effects were calculated according to Equation 4 and were graphed against their respective Ca^{2+} concentration. Thio effects for both stereoisomers remained relatively consistent over difference concentrations of Ca^{2+} indicating a lack of a significant thio effect.

To determine if general acid/base catalysis was occurring, kinetic tests were conducted using SDIE on UpG hydrolysis. To determine the rate of the reaction, the fraction of UpG remaining of an aliquot was graphed against time and fit to single exponential decay using KaleidagraphTM. A normal SDIE, >1 , or no SDIE was expected to occur referring to either general acid or general base catalysis. Instead what was

observed was an inverse SDIE, where the SDIE was less than one. Figure 23 depicts one experiment where the reaction in D₂O had a rate constant of 0.047 and a reaction in H₂O had a rate constant of 0.042.

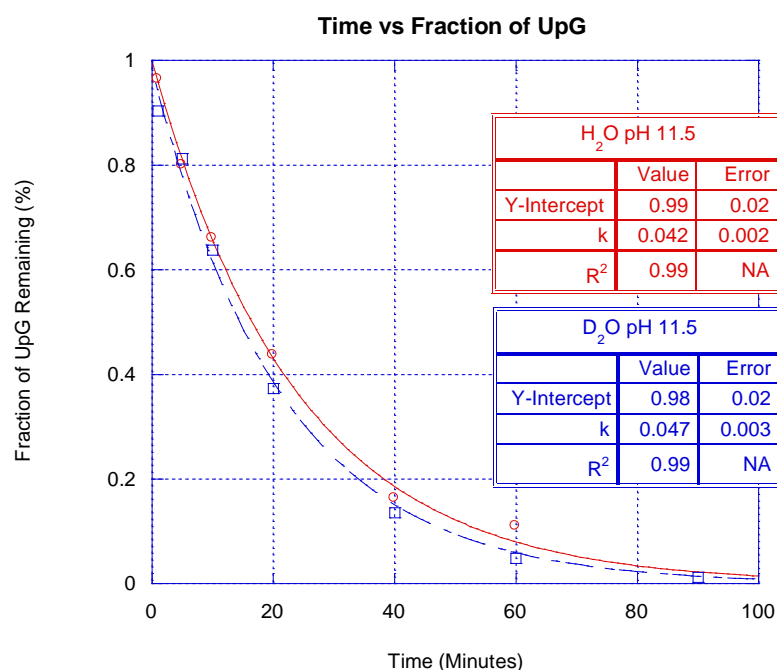


Figure 23: Fraction of UpG remaining against time elapsed in neutralized 60 μ L aliquot containing 0.33M Ca²⁺ at pH 11.5 and 37^oC with a ionic strength of 1 and either H₂O(red) or D₂O(blue). Each line is fit to an exponential fit and represents a different concentration trial. When comparing the H₂O to the D₂O trials an inverse SDIE is observed

This was observed in all trials and the average rate constant, k , was calculated for H₂O and D₂O trials. (Table 2) The average rate constant of H₂O trials was 0.035 ± 0.002 and the average rate constant of D₂O trials was 0.048 ± 0.003 . Equation 3 was used to calculate the SDIE for each set of experiments and the average SDIE was calculated to be 0.74 ± 0.053 . This results in an average inverse SDIE for Ca²⁺ catalyzed phosphodiester hydrolysis indicating neither general acid or general base catalysis.

Table 2:UpG Solvent Deuterium Isotope Effects For UpG Cleavage			
	$k_{\text{H}_2\text{O}}(\text{min}^{-1})$ NaOH	$k_{\text{D}_2\text{O}}(\text{min}^{-1})$ NaOH	SDIE NaOH
Average	0.035	0.048	0.735
Std Dev	0.002	0.003	0.053

The original trials were conducted using NaOH to maintain the pH and the experiment was later repeated using a CAPS buffer system. The average SDIE of the CAPS buffer systems was equal to 0.699 with a standard deviation of 0.011, not shown in Table 2.

(Yasin and Cassano, unpublished results)

Discussion

Proposed Catalytic Mechanism for Ca²⁺ Catalysis

Although the exact mechanism of Ca²⁺ catalyzed RNA phosphodiester hydrolysis has not been determined, the number of possible mechanisms has been narrowed down significantly for the UpG model. The saturation behavior displayed by k_{obs} vs Ca²⁺ plot, Figure 19, is consistent with a model depicting the association of Ca²⁺ and UpG previous to nucleophilic attack. Mg²⁺ studies with DNA show the same phenomena and conclude that the saturating nature is consistent with the formation of a complex previous to nucleophilic attack. (Kirk 2010) The saturating model is also consistent with the association of one Ca²⁺ in a complex with UpG previous to cleavage.

It was suspected that the Ca²⁺ catalytic mechanism involved general acid or general base catalysis. These have been observed in previous models systems where the introduction of a Zn²⁺ ion to the system caused an increase in the B_{LG} value from -1.28 to

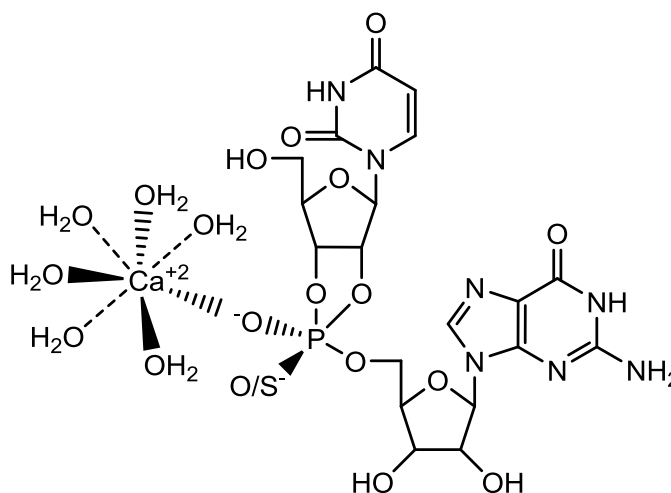


Figure 24: Mechanism of Ca²⁺ catalyzed RNA phosphodiester hydrolysis of phosphorothioate model. The current hypothesis suggests that coordination of Ca²⁺ to the non-bridging oxygen atoms can occur in the presence of only 1 oxygen atom and acts as a Lewis acid to stabilize the growing negative charge upon formation of the phosphorane intermediate.

-0.32. (Mikkola 1999) This was indicative of Zn^{2+} inducing catalysis through a general acid mechanism in which a proton was donated to the leaving group. The large negative B_{LG} suggests that negative charge accumulates on the leaving group suggesting the formation of an alkoxy ion. Upon introduction of the Zn^{2+} ion, an increase in the B_{LG} occurs which suggests that less negative charge develops on the alkoxy group. (Mikkola 1999) This is indicative of protonation occurring on the alkoxy group which can be attributed to the participation of the Zn^{2+} in a general acid mechanism. So it is hypothesized that metal ions can participate in a general acid mechanism during phosphodiester hydrolysis. SDIE were utilized to determine if proton transfer occurred during the reaction by replacement of the water solvent with a deuterated water solvent and comparison of the reaction rates. The SDIE confirm that Ca^{2+} forms a complex previous to nucleophilic attack. SDIE were used specifically to determine if Ca^{2+} catalyzed phosphodiester hydrolysis of UpG proceeded by general acid or general base catalysis. The lack of a normal (>1) SDIE suggests that neither general acid nor general base catalysis occurs. (Table 2) This indicates that electrostatic interactions between the positive Ca^{2+} and negative phosphate are the dominant force in catalysis.

This prompted the use of kinetic tests to see if the mechanism of Ca^{2+} involved the metal ion as a Lewis acid and stabilization of the phosphorane. The Korhonen 2013 study looked at a variety of alkyl esters in various reaction conditions to determine the effects of metal ion catalysis. It was observed that the B_{LG} values of the Zn^{2+} catalyzed reaction of an alkyl phosphate were similar to those of a nucleoside 3'phosphotriester under neutral conditions. (Korhonen 2013) It was concluded that the mechanisms are

similar and so the Zn^{2+} catalyzed reaction must proceed with the Zn^{2+} neutralizing the charge on the phosphate and allowing for stabilizing the phosphorane.

Kinetic tests were performed with a thiosubstituted UpG model in order to determine if Ca^{2+} was associating with the non-bridging oxygen atoms, Figure 21. Ca^{2+} is a hard Lewis acid and so should have a higher affinity for oxygen than for sulfur. Therefore if Ca^{2+} is associating with the non-bridging oxygen, the thiosubstituted model should experience a loss in affinity and/or a loss in k_{max} relative to the phosphodiester UpG model. Table 1 summarizes what is observed for the kinetic studies with the non-thiosubstituted and the thiosubstituted models. The rate difference observed between the non-thiosubstituted and thiosubstituted model appear somewhat different to previous studies. In a 1979 study conducted by Burgers, et al the RNA model UpA and the thiosubstituted UpA models were utilized in experiments with ribonucleases and a phosphodiesterase from snake venom. The rate constants were observed in only the presence of 0.5M KOH and this resulted in a thio effect of 1.32 for the R_P isomer and 1.06 for the S_P isomer. (Burgers 1979) For UpG and UpsG, the average thio effect for the R_P isomer was 3.73 and for the S_P isomer 1.37. The difference in rate constant for the S_P isomer could probably be explained by the large standard deviation in the rate constants for in this study resulting in some error. The difference in rate constant for the R_P isomer is interesting due to the large difference in magnitude and is harder to comment on without further information. Both the current and past study seem to indicate that the R_P isomer has a larger deficit in the rate constant when compared to the S_P isomer.

Due to no difference between the K_D values of the non-thiosubstituted and thiosubstituted models and small normal thio effects observed, Figure 22, Ca^{2+} may not be associating with non-bridging oxygen atoms. Yet comparisons to previous studies indicate that the observed thio effects are within a range that is typical for monosubstituted RNA models and suggest that the Ca^{2+} does not act directly with the non-bridging oxygen atoms but through less direct electrostatic stabilization. (Ora, 1998) The previous study determined that for hard metal ions, specifically Mn^{2+} and Mg^{2+} , either no thio effect was observed or up to an 8-fold decrease in rate constant was observed. (Ora 1998) The researchers inferred this as interruption to the coordination of the metal ions to the RNA model, especially since softer metal ions, such as Cd^{2+} and Gd^{3+} , showed significant rate constant increases up to 3,600 fold with the thio-substituted models. (Ora 1998) This means that Ca^{2+} could still be coordinating with the phosphorane intermediate but further experimentation would be needed to confirm the coordination of the Ca^{2+} with the non-bridging oxygen atoms due to the lack of significant thio effects.

Further literature research has yielded that a stereoselective mechanism can cause a large deficit in rate for Ca^{2+} catalysis of RNA phosphodiester hydrolysis. In a previous enzymatic study it was noted that a stereoselective reaction occurred where Ca^{2+} interacted with one non-bridging oxygen atom. (Zhao 2002) Upon substitution of that oxygen with a sulfur atom, a significant decrease in the rate constant occurred, a 1.6×10^8 fold decrease. (Zhao 2002) Substitution of the other oxygen resulted in a 47-fold decrease in rate constant indicating that the reaction was stereoselective. (Zhao 2002) The enzyme, phospholipase C, had several amino acid residues that directed and

coordinated the Ca^{2+} with a specific non-bridging oxygen atom; thus when that oxygen was substituted a significant thio effect was seen. (Zhao 2002) With the UpG model of Ca^{2+} catalyzed phosphodiester hydrolysis, there is no mechanism or structural constraint that can force the interaction of Ca^{2+} with one specific oxygen atom. Thus it is hypothesized that the Ca^{2+} could interact with the remaining oxygen atom in the thiosubstituted model. This would result in a slight decrease in the affinity and have a minimal effect on the rate constant and V_{\max} .

A small effect on affinity when additional oxygen atoms are available can be seen in other model systems such as adenosine-5'-O-phosphate where the introduction of a sulfur molecule into the non-bridging position does not interrupt the binding of Ca^{2+} . (Sigel 1997) Instead equal binding properties are observed presumably since the Ca^{2+} associates with the two non-bridging oxygen atoms instead of associating with the sulfur substituted atom. (Sigel 1997) The new hypothesis, where Ca^{2+} can associate either non-bridging oxygen for catalysis but association with both non-bridging oxygen atoms is necessary for maximum catalysis, does have a theoretical basis. In order to further test this hypothesis, the use of a disubstituted model has been proposed where both non-bridging oxygen atoms have been replaced with a sulfur atom. In this situation, if Ca^{2+} is associating with the non-bridging oxygen atoms, the lack of oxygen atoms should be able to fully disrupt the binding of Ca^{2+} to the phosphorane intermediate and significantly impact both the affinity and rate of reaction, Figure 24.

Comparison With Ca^{2+} Catalysis of DNA Models

The UpG rate constant hydrolysis plot represents a surprising departure from those of the DNA rate constant plot vs Ca^{2+} from the Kirk et al, study (2010). In this

study a DNA model called thymidine-5'-p-nitrophenyl phosphate, T5PNP, was utilized. The main difference between the UpG RNA model and the T5PNP DNA model is that the leaving group of the UpG model is poor compared to the T5PNP model which has a very good leaving group. The kinetic trials conducted by Kirk et al with T5PNP and Ca^{2+} showed a quadratic relationship at low concentrations but higher concentrations began to display saturation behavior. (Kirk 2010) The T5PNP plot can be described as one that has upward curvature at low Ca^{2+} concentrations and then has downward curvature at high Ca^{2+} concentrations. (Kirk 2010) As opposed to the RNA rate constant plot in which downward curvature is seen and displays only saturation behavior. (Figure 21) This suggests that Ca^{2+} catalyzed RNA phosphodiester hydrolysis proceeds by a mechanism that differs from Ca^{2+} catalyzed phosphodiester hydrolysis of T5PNP. Where the T5PNP Ca^{2+} curve suggests a model of catalysis that is described as a one and two metal ion parallel catalytic mechanism and the RNA Ca^{2+} curve suggests a one metal ion mechanism. (Kirk 2010)

There is also a large discrepancy between the Ca^{2+} RNA energetics and the Ca^{2+} T5PNP energetics. The DNA fit yielded a rate (k) equal to $1 \times 10^{-3} \text{ M}^{-1}\text{s}^{-1}$ for one Ca^{2+} ion and for two Ca^{2+} ions the rate was equal to $1 \times 10^{-2} \text{ M}^{-1}\text{s}^{-1}$. (Kirk 2010) Kirk calculates that these rates are equal to 90 and 900 fold catalysis with a total $\ddagger\text{G}$ contribution of 18 kJ/mol and a contribution of 12 kJ/mol for the first ion and 6 kJ/mol for the second ion. (Kirk 2010) The Ca^{2+} catalyzed RNA phosphodiester hydrolysis had a 326-fold increase in rate with a $\ddagger\text{G}$ of 14.5 kJ/mole. If RNA Ca^{2+} catalyzed hydrolysis occurred with the same mechanism as DNA Ca^{2+} catalyzed hydrolysis, similar values would be observed. What is seen are significant differences in the rate with the metal ion

catalysis of RNA lying in between single and double metal catalysis of the DNA model. When comparing the fold increase in rate for the one and two metal catalysis of the DNA model, the fold increase for RNA is about 3.6 times larger than one Ca^{2+} catalysis and about 3 times smaller than the two Ca^{2+} mechanism. Accordingly the $^{\ddagger}\text{G}$ values are about 2 kJ/mole smaller or 4 kJ/mole larger with one or two Ca^{2+} ions, respectively. Such large differences reinforce the conclusions drawn from the plots; that RNA Ca^{2+} catalyzed phosphodiester hydrolysis does not proceed with a parallel single and double ion mechanism.

Bibliography

- Beese LS, Steitz TA. 1991. *Structural basis for the 3' 5' exonuclease activity of Escherichia coli DNA polymerase I: a two metal ion mechanism*. The EMBO Journal 10: 25-33.
- Beurdeley M, et al. 2013. *Compact designer TALENs for efficient genome engineering*. Nature Communications. 4: 1762.
- Blackburn GM, Gait, MJ. *Nucleic Acids in Chemistry and Biology*. Oxford University Press. New York. 1990. p 446.
- Bonfa L, Gatos M, Mancin F, Tecilla P, Tonellato U. 2003. *The Ligand Effect on the Hydrolytic Reactivity of Zn(II) Complexes toward Phosphate Diesters*. Inorganic Chemistry. 42: 3943-3949.
- Burgers PMJ, Eckstein F. 1979. *Diastereomers of 5'-O- Adenosyl 3'-O-Uridyl Phosphorothioate: Chemical Synthesis and Enzymatic Properties*. American Chemical Society. 18: 592- 596
- Cassano AG, Anderson VE, Harris ME. 2002. *Evidence for Direct Attack by Hydroxide in Phosphodiester Hydrolysis*. J. Am. Chem. Soc. 124: 10964-10965.
- Cassano AG, Anderson VE, Harris ME. 2004. *Analysis of Solvent Nucleophile Isotope Effects: Evidence for concerted Mechanisms and Nucleophilic Activation by Metal Coordination in Nonenzymatic and Ribozyme-Catalyzed Phosphodiester hydrolysis*. Biochemistry. 43: 10547-10559
- Chen JH, et al. 2010. *A 1.9 Å Crystal Structure of the HDV Ribozyme Precleavage Suggests both Lewis acid and General Acid Mechanisms Contribute to Phosphodiester Cleavage*. Biochemistry. 49: 6508-6518

- Chen J, Ganguly A, Miswan Z, Hammes-Schiffer S, Bevilacqua PC, Golden B. 2013. *Identification of the catalytic Mg²⁺ Ion in the Hepatitis Delta Virus Ribozyme*. ACS Biochemistry. 52: 557-567.
- Dahm SC, Derrick WB, Uhlenbeck OC. 1993. *Evidence for the Role of Solvated Metal Hydroxide in the Hammerhead Cleavage Mechanism*. American Chemical Society. 32: 13040-13045
- Feng G, Natale D, Prabakaran R, Mareque-Rivas JC, Williams NH. 2006. *Efficient Phosphodiester Binding and Cleavage by a Zn^{II} Complex Combining Hydrogen Bonding Interactions and Double Lewis acid Activation*. Angew. Chem Int. Ed. 45: 7056-7059.
- Golden BL. 2011. *Two Distinct Catalytic Strategies in the Hepatitis Delta Virus Ribozyme Cleavage Reaction*. Biochemistry. 50: 9424-9433
- Harris ME, Dai Qing, Gu Hong, Kellerman DL, Piccirilli JA, Anderson VE. 2010. *Kinetic Isotope Effects for RNA Cleavage by 2'-O-Transphosphorylation: Nucleophilic Activation by Specific Base*. J. Am. Chem. Soc. 132: 11613-11621.
- Hengge AC, Cleland WW. 1991. *Phosphoryl-Transfer Reactions of Phosphodiester: Characterization of Transition States by Heavy-Atom Isotope Effects*. J. Am. Chem. Soc. 113: 5835-5841.
- Holtz KM, Kantrowitz ER. 1999. *The mechanism of the alkaline phosphatase reaction: insights from NMR, crystallography and site-specific mutagenesis*. FEBS Letters. 462: 7-11.

- Humphry T, Forconi Marcello, Williams NH, Hengge. 2002. *An Altered Mechanism of Hydrolysis for a Metal-complexed Phosphate Diester*. J. Am. Chem. Soc. 124: 14860-14861.
- Humphry T, Iyer S, Iranzo Olga, Morrow JR, Richard JP, Paneth P, Hengge AC. 2008. *Altered Transition State for the Reaction of an RNA Model Catalyzed by a Dinuclear Zinc(II) Catalyst*. J. Am. Chem. Soc. 130: 17858-17866.
- Imohof P, Fischer S, Smith JC. 2009. *Catalytic Mechanism of DNA Backbone Cleavage by the Restriction Enzyme EcoRV: A Quantum Mechanical/Molecular Mechanical Analysis*. Biochemistry. 48: 9061-9075.
- Kirk BA, et al. 2010. *Mononuclear and dinuclear mechanisms for catalysis of phosphodiester cleavage by alkaline earth metal ions in aqueous solution*. Journal of Inorganic Biochemistry. 104: 207-210.
- Ku WY, Liu YW, Hsu YC, Liao CC, Liang PH, Yuan HS, Chak KF. 2002. *The zinc ion in the HNH motif of the endonuclease domain of colicin E7 is not required for DNA binding but is essential for DNA hydrolysis*. 30: 1670-1678.
- Korhonen H, Williams NH, Mikkola S. 2013. *β_{LG} values in mechanistic studies on the transesterification of RNA models and their application in a metal ion complex promoted transesterification*. J. Phys. Org. Chem. 26: 182-186.
- Lassila JK, Zalatan JG, Herschlag. 2011. *Biological Phosphoryl-Transfer Reactions: Understanding mechanism and Catalysis*. Annu. Rev. Biochem. 80: 669-702.
- Liang J, Canary JW. 2010. *Discrimination between Hard Metals with Soft Ligand Donor Atoms: An On-Fluorescence Probe for Manganese(II)*. Angew. Chem. Int. Ed. 49: 7710-7713.

- Mannino SJ, Jenkins CL, Raines RT. 1999. *Chemical Mechanism of DNA Cleavage by the Homing Endonuclease I-PpoI*. *Biochemistry*. 38: 16178-16186.
- Mikkola S, Stenman E, Nurmi K, Yousefi-Salakdeh E, Strömberg R, Lönnberg H. 1999. *The mechanism of the metal ion promoted cleavage of RNA phosphodiester bonds involves a general acid catalysis by the metal aquo ion on the departure of the leaving group*. *J. Chem. Soc., Perkin Trans. 2*: 1619-1625.
- Murtola M, Stromberg R. 2008. *PNA based artificial nucleases displaying catalysis with turnover in the cleavage of a leukemia related RNA model*. *Org Biomol. Chem.* 6: 3837-3842.
- Mussolino C, Cathomen T. 2012. *TALE nucleases: tailored genome engineering made easy*. *Current Opinion in Biotechnology*. 23: 644-650
- NIST [National Institute of Standards and Technology]. 2011. Gaunosine.
<http://webbook.nist.gov/cgi/cbook.cgi?Formula=C10H13N5O5&NoIon=on&Units=SI>.
- Nowotny M, Gaidamakov SA, Crouch RJ, Yang W. 2005. *Crystal Structures of RNase H Bound to an RNA/DNA Hybrid: Substrate Specificity and Metal-Dependent Catalysis*. *Cell*. 121: 1005-1016.
- Ora M, Peltomaki M, Oivanen M, Lonnerberg H. 1998. *Metal-Ion-Promoted cleavage, Isomerization, and Desulfurization of the Diastereomeric Phosphoromonothioate analogues of uridylyl(3',5') Uridine*. *J. Org. Chem.* 63: 2939-2947.
- Pinjari RV, Kaptan SS, Gejji SP. 2008. Alkali metals (Li, Na, and K) in methyl phosphodiester hydrolysis. *Phys. Chem. Chem. Phys.* 11: 5253-5262

- Purcell J, Hengge AC. 2005. *The Thermodynamics of Phosphate versus Phosphorothioate Ester Hydrolysis*. J. Org. Chem. 2005. 70: 8437- 8442
- Rawlings J, Cleland WW, Hengge AC. 2006. *Metal-Catalyzed Phosphodiester Cleavage: Secondary ^{18}O Isotope Effects as an Indicator of Mechanism*. J. Am. Chem. Soc. 128: 17120-17125.
- Sigel RKO, Song B, Sigel H. 1997. *Stabilities and Structures of Metal Ion Complexes of Adenosine 5'-O-Thiomonophosphate (AMPS $^{2-}$) in Comparison with Those of Its Parent Nucleotide (AMP $^{2-}$) in Aqueous Solution*. J. Am. Chem. Soc. 119: 744-755
- Schroeder GK, Lad C, Wyman P, Williams NH, Wolfenden R. 2005 *The time required for water attack at the phosphorus atom of simple phosphodiester and of DNA*. PNAS. 103: 4052-4055.
- Viratanen N, Polari L, Valila M, Mikkola S. 2005. *Kinetic solvent deuterium isotope effect in transesterification of RNA models*. J. Phys. Org. Chem. 18: 385-397.
- Westheimer FH. 1987. *Why Nature Chose Phosphates*. Science. 235: 1173-1178
- Wong KY, Lee TS, York DM. 2011. *Active Participation of the Mg $^{2+}$ Ion in the Reaction Coordinate of RNA Self-Cleavage Catalyzed by the Hammerhead Ribozyme*. J. Chem. Theory Comput. 7: 1-3
- Wong KY, Lee TS, York DM. 2011. *Active Participation of the Mg $^{2+}$ Ion in the Reaction Coordinate of RNA Self-Cleavage Catalyzed by the Hammerhead Ribozyme*. J. Chem. Theory Comput. 7: 1-3.
- Zhao L, Liu Y, Bruzik KS, and Tsai MD. 2002. *A Novel Calcium-Dependent Bacterial Phosphatidylinositol-Specific Phospholipase C Displaying Unprecedented*

Magnitudes of Thio Effect, Inverse Thio Effect, and Stereoselectivity. J. Am. Chem. Soc. 125: 22-23

Zhao L. 2003. *Mechanistic Studies on Phosphatidylinositol-Specific Phospholipase C.* Ohio State University. 135p.